The Hadronic Structure of the Photon

(Two Photon Physics at LEP)

Chih-Hsun LIN
NCU, Taiwan

- Cross-section of $\gamma\gamma$ collisions
  - Inclusive charged particle production
  - $\rho^0 - \rho^0$ scattering
- Inclusive charm production in $\gamma\gamma$ collisions
- Photon Structure Function
  - Hadronic F_2^γ → low x
  - Leptonic F_2^γ → Azimuthal Correlations (F_L)
- Cross-section of $\gamma^*\gamma^*$ collisions
  - Search for BFKL Pomeron

September 11 1998

Kinematics

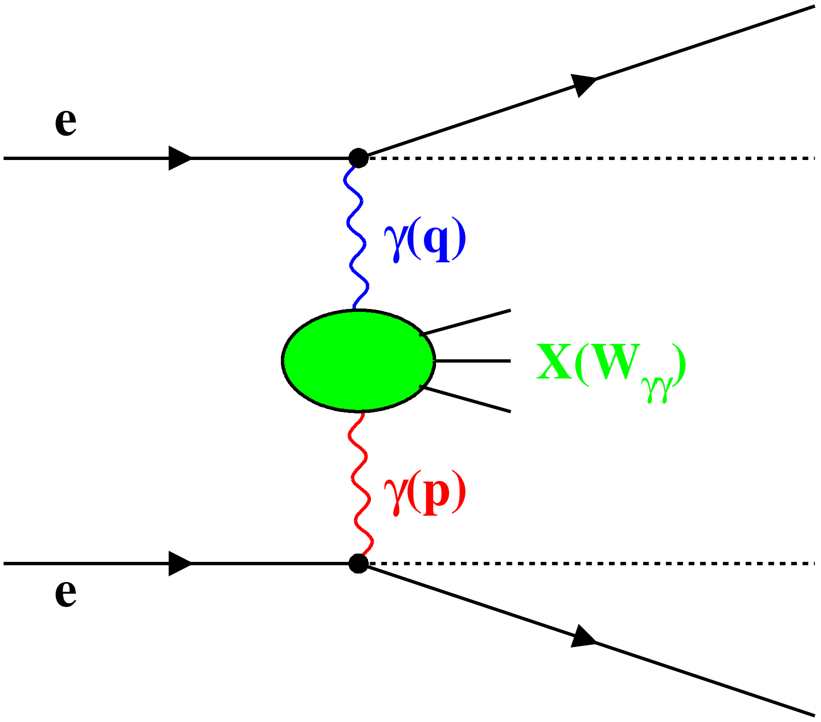

- The virtualities of photons:
  $Q^2 = -q^2 \quad , \quad P^2 = -p^2$

- $W_{\gamma\gamma} = \sqrt{(p+q)^2}$ is the $\gamma\gamma$ centre-of-mass energy.

- The final state X can be :
  1. A single resonant state
  2. Lepton pairs
  3. A non-resonant hadronic state

The two-photon events can be classified as:

1. Non-tagged events ($Q^2 \sim P^2 \sim 0$)
   - Both scattered $e^{\pm}$ are lost in the beam pipe.
     - ⇨ Both photons are quasi-real.
   - We can study :
     - ⇨ σ_{tot} of $\gamma\gamma$ collisions
     - ⇨ Inclusive Charm production
     - ⇨ Vector meson scattering ($\gamma\gamma \to \rho^0\rho^0$)
     - ⇨ Resonance properties and new resonances (Glueballs) ➜ not included in the talk.

2. Single-tagged events ($Q^2 >> P^2 \sim 0$)
   - Only one scattered electron is detected.
     - ⇨ One photon is highly virtual and the other is quasi-real.
     - ⇨ Q^2 is well measured.
   - We can study :
     - ⇨ Photon structure functions
     - ⇨ The photon-meson transition form factor

Two-photon events

3. Double-tagged events

- Both scattered electrons are detected.
  - Q^2 and P^2 are well measured.
  - $W_{\gamma\gamma}$ can be measured directly → No unfolding
- We can study :
  - Cross-section of $\gamma^*\gamma^*$ collision → BFKL Pomeron
  - Virtual photon structure function

Two-Photon Physics at LEP

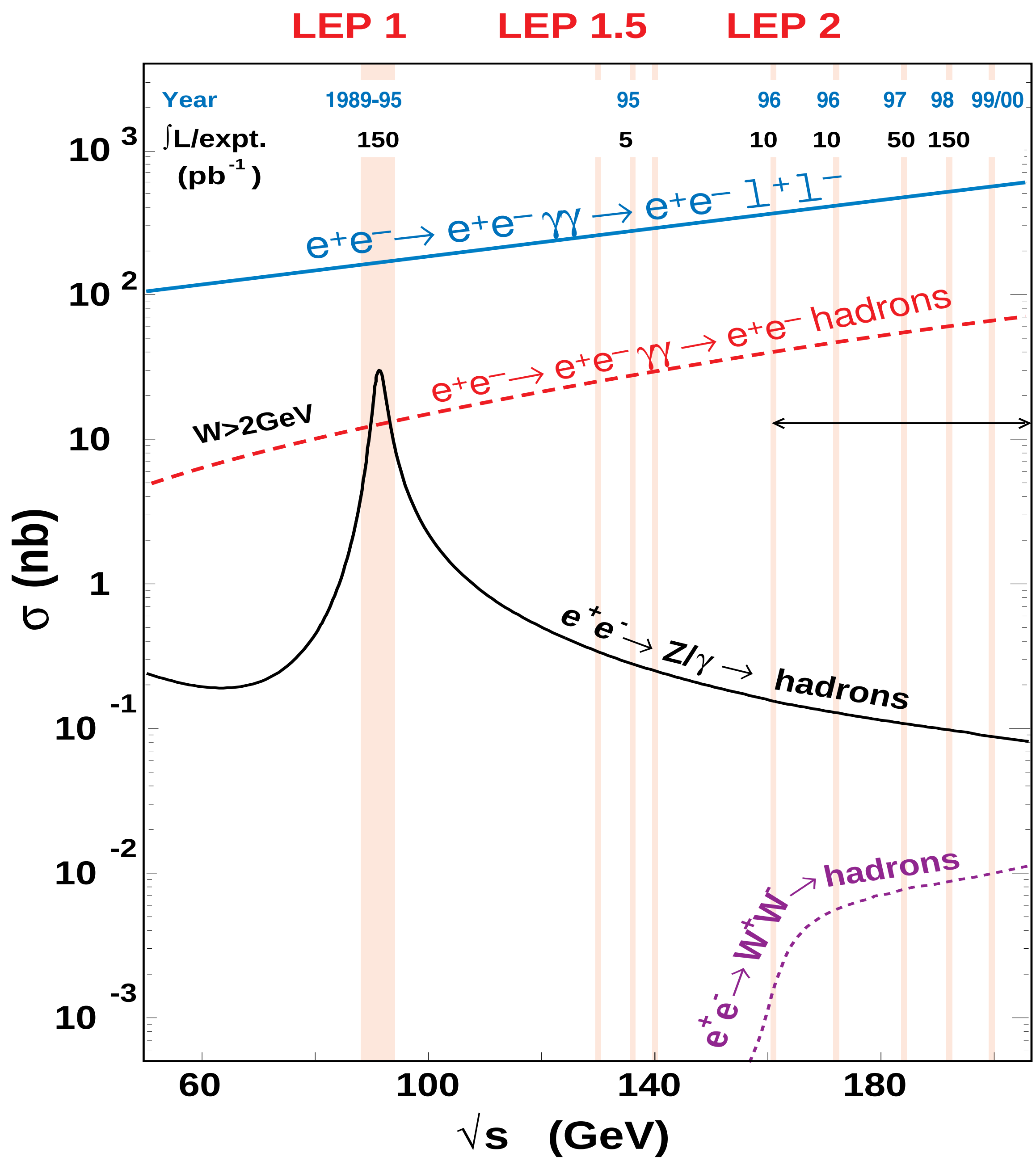

- ❑ The dominant interaction at **LEP2** is the **Two-photon processes**.
- ❑ **LEP2** is the best place to study two-photon physics (**high cross-section, low background**).

The measurements before LEP :

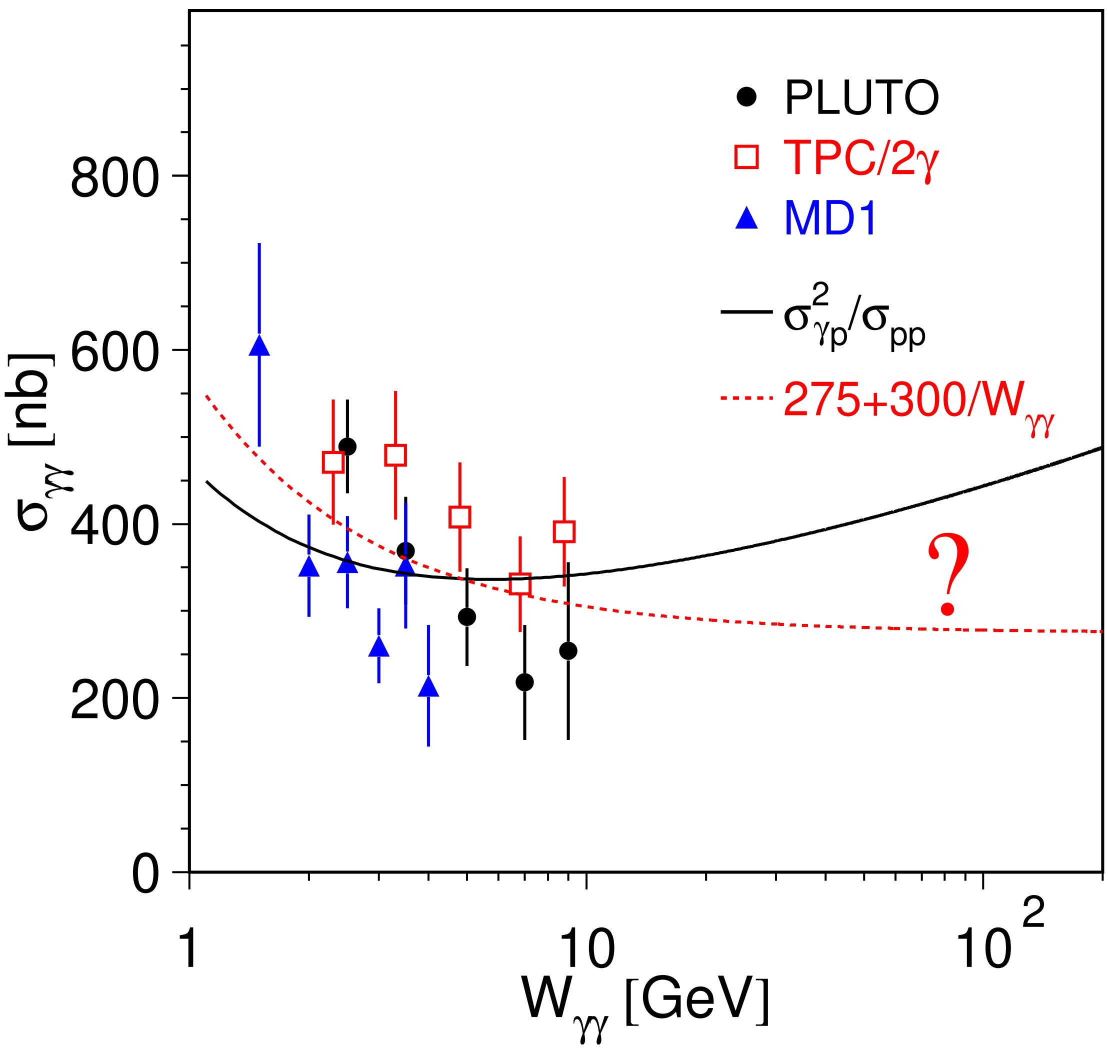

- limited by beam energy ➜ $W_{\gamma\gamma} < 10$ GeV.
- very wide spread in the measurements.
- Does $\sigma_{\gamma\gamma}$ increase at high energy ?
- At LEP, 5 GeV $< W_{\gamma\gamma} <$ 145 GeV has been measured.

Total $\sigma_{\gamma\gamma}$: Physics

The diagrams contributing to :

$$e^+e^- \rightarrow e^+e^-\gamma\gamma \rightarrow e^+e^-\text{hadrons}$$

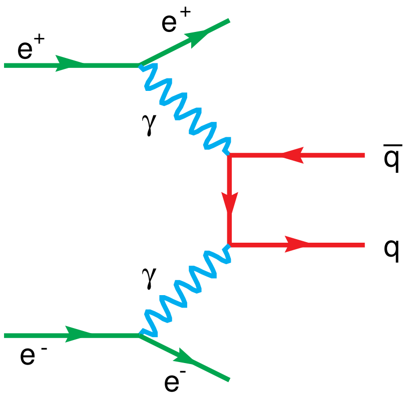

Direct

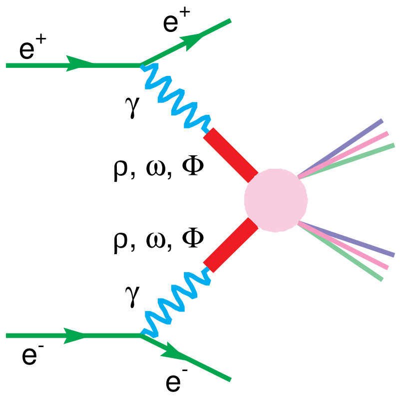

VDM

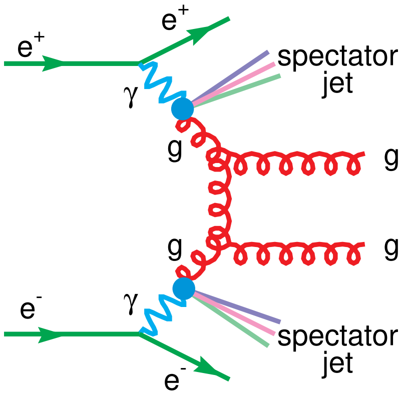

Double Resolved

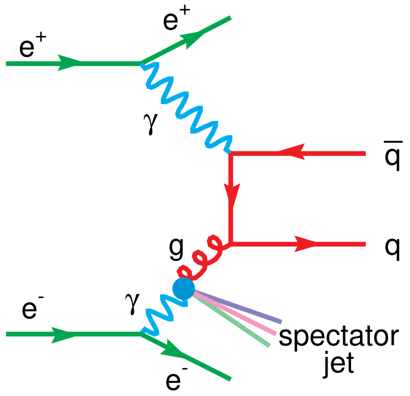

Single Resolved

➩ **The VDM process is dominant.**

Total $\sigma_{\gamma\gamma}$: Analysis

- Data :

L3 :	91 GeV,	140. pb^{-1}
	130 - 140 GeV,	4.98 pb^{-1}
	161 GeV,	10.4 pb^{-1}
	183 *GeV*,	51.9 pb^{-1}
	189 *GeV*,	21.6 pb^{-1}

OPAL: $161 - 172$ *GeV*, 19.9 pb^{-1}

- Monte Carlo :

PHOJET: R. Engel and J. Ranft.
(Phys. Rev. D54, 4246, 1996)

PYTHIA: T. Sjöstrand
(CPC 82, 74, 1994)

- Due to detector effect ➜ $W_{vis} < W_{\gamma\gamma}$

  ➩ Use unfolding for $W_{vis} \rightarrow W_{\gamma\gamma}$

  ➩ Need good Monte Carlo

L3 preliminary

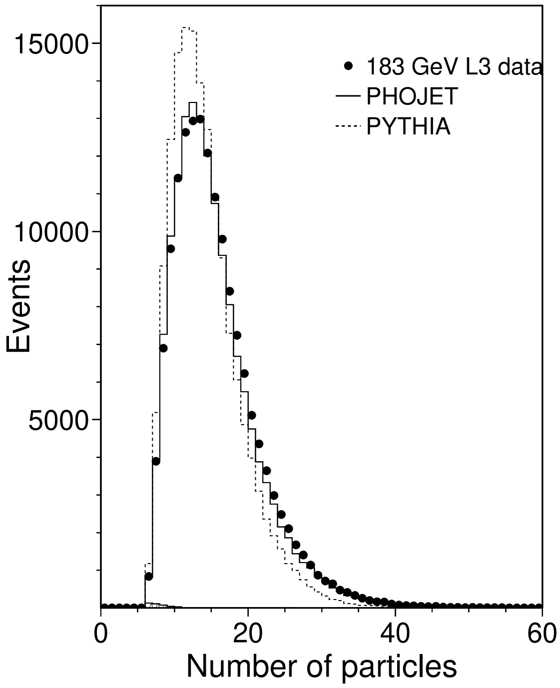

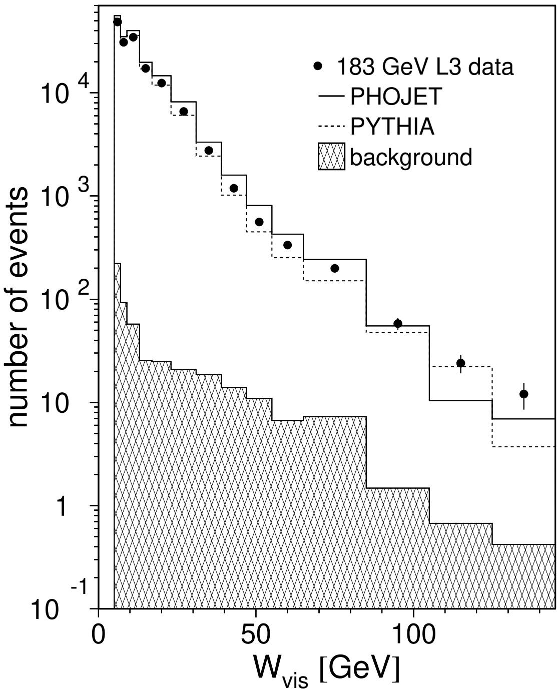

*particles = charged particles + photons

OPAL preliminary

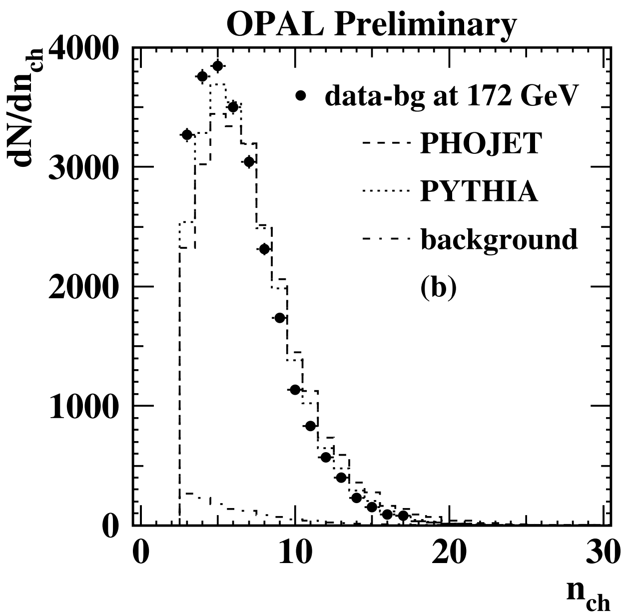

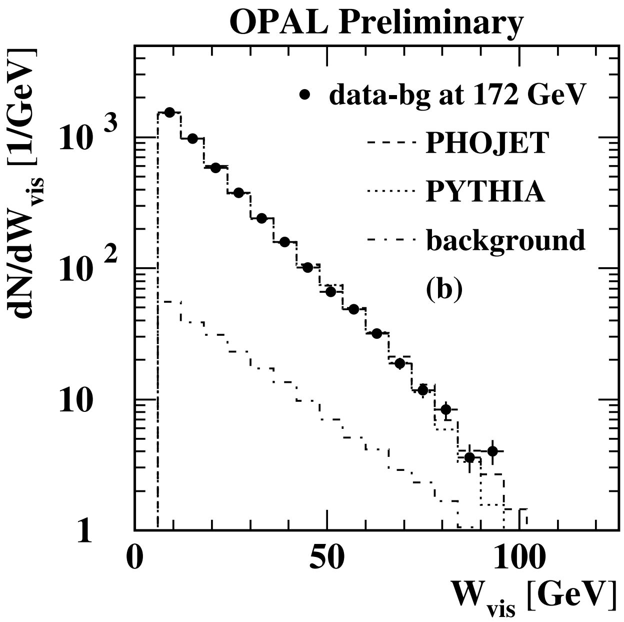

*ch = charged particles

Total $\sigma_{\gamma\gamma}$: $d\sigma_{ee} \rightarrow \sigma_{\gamma\gamma}$

❑ $d\sigma(\mathrm{e^+e^-} \rightarrow \mathrm{e^+e^-hadrons})$

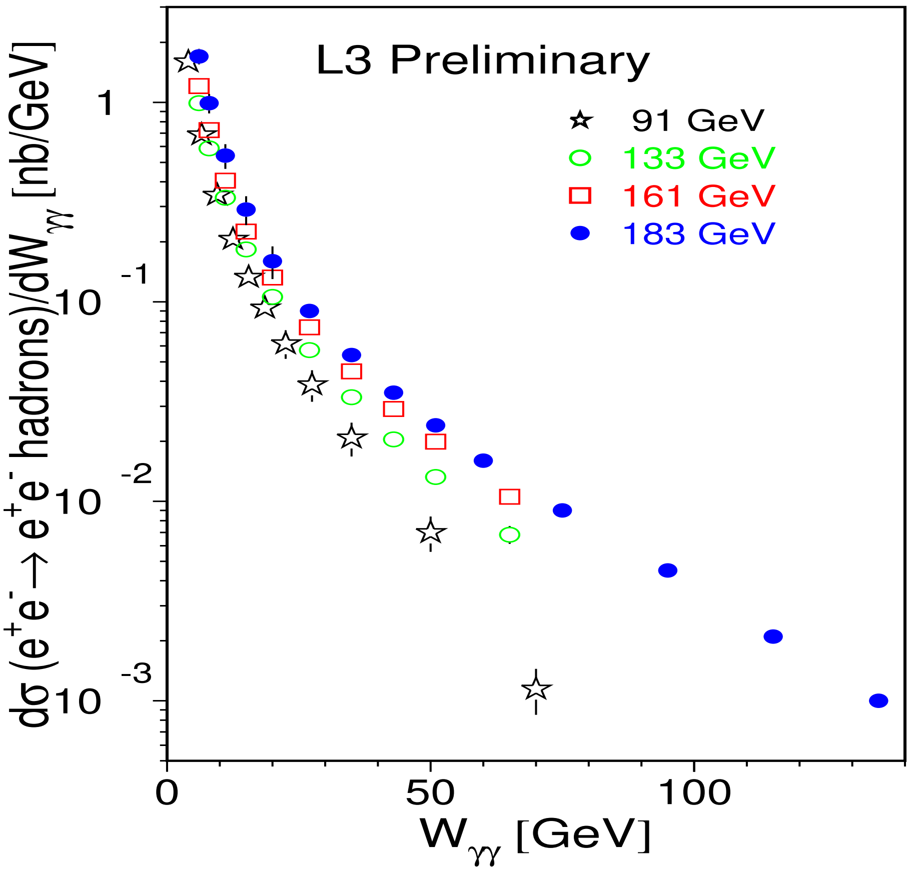

✻ Effect of the $\gamma\gamma$ luminosity function

➜ $d\sigma_{ee}$ increases with increasing beam energy.

➜ $d\sigma_{ee}$ decreases with increasing $W_{\gamma\gamma}$.

❑ Extract $\sigma_{\gamma\gamma}$ from $d\sigma_{ee}$

$$\frac{d\sigma_{ee}}{d(W^2_{\gamma\gamma}/s)} = \int \frac{dQ^2}{Q^2}\frac{dP^2}{P^2} \sum_{a,b=T,S} \mathcal{L}_{ab}\sigma^{\gamma\gamma}_{ab}(W_{\gamma\gamma}, P^2, Q^2)$$

$$\sigma^{\gamma\gamma}_{ab}(W_{\gamma\gamma}, P^2, Q^2) = F_a(Q^2)F_b(P^2)\sigma^{\gamma\gamma}_{ab}(W_{\gamma\gamma})$$

*T and S are Transverse and Scalar photon helicity indices.

➩ $\sigma^{\gamma\gamma}_{TT}$ is dominant.

➩ Remove the effect of $\mathcal{L}$ and $F(Q^2, P^2)$ ➜ $\sigma_{\gamma\gamma}(W_{\gamma\gamma})$

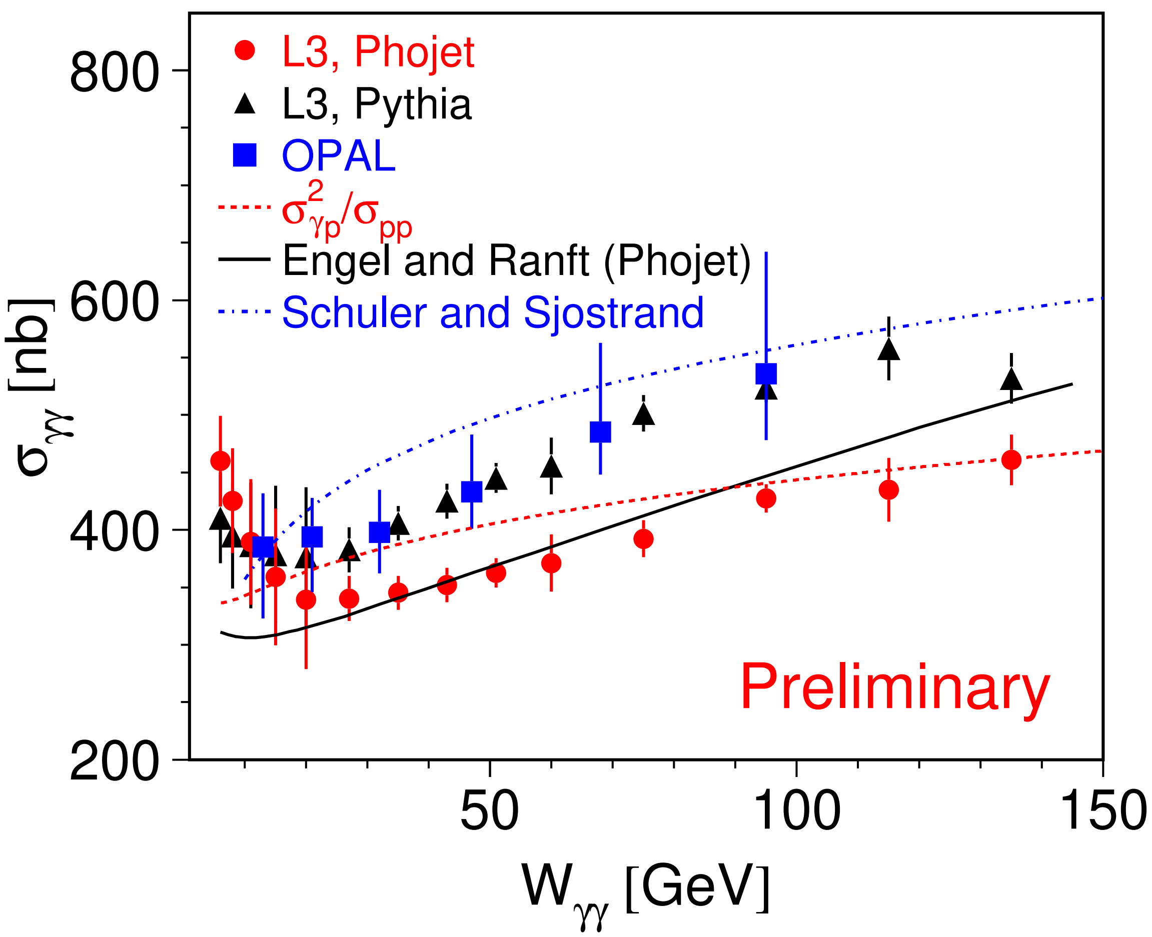

- The systematic error of L3 is experimental error only.
- The values of OPAL is the average of results obtained with Phojet and Pythia.
  The difference is included in the systematic error shown.
- Both OPAL and L3 show clear rising behaviour with increasing energy. ➩ Independent of MC
- The uncertainty on absolute values is large ($\sim$ 20%).
  ➩ Due to the MC model dependence.
- L3 and OPAL are compatible with same generator (PYTHIA).

Total $\sigma_{\gamma\gamma}$: DL fit

- Fit with Donnachie and Landshoff parametrisation :
  (*Phys. Lett., B296, 227, 1992)

$$\sigma_{\gamma\gamma} = As^{\varepsilon} + Bs^{\eta} \ , \ \ s = W^2_{\gamma\gamma}$$

Using the universal values of $\eta = -0.4678$ (PDG 96)

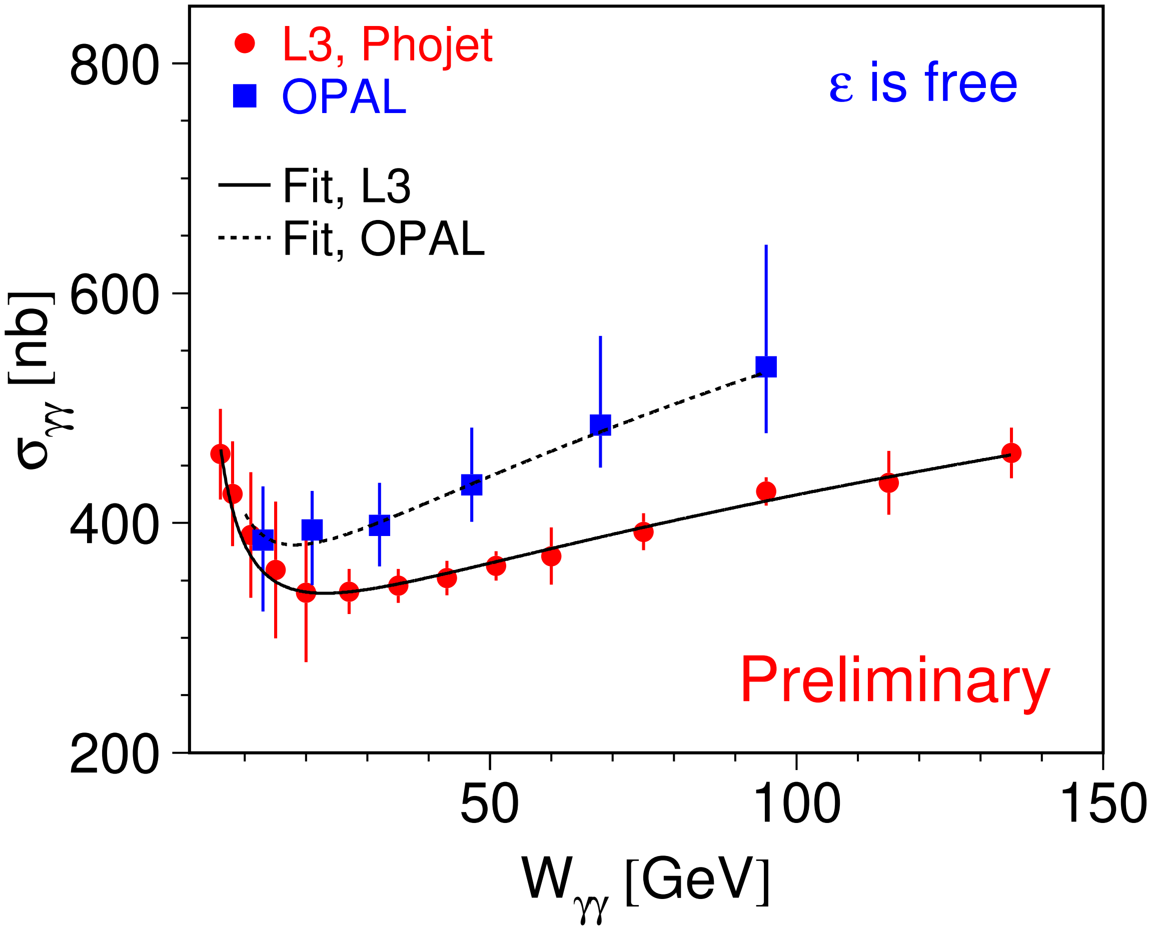

L3 : $\varepsilon = 0.158 \pm 0.006(stat) \pm 0.028(sys)$

OPAL : $\varepsilon = 0.19 \pm 0.09$

PDG 96 : $\varepsilon = 0.0790 \pm 0.0011$

- ⇨ a factor of two higher !
- ⇨ contribution from another Pomeron ?!
  (hard Pomeron)

Total $\sigma_{\gamma\gamma}$: 189 GeV data

➜ New measurements at 189 GeV ($\mathcal{L} = 21.6\ \mathrm{pb}^{-1}$)

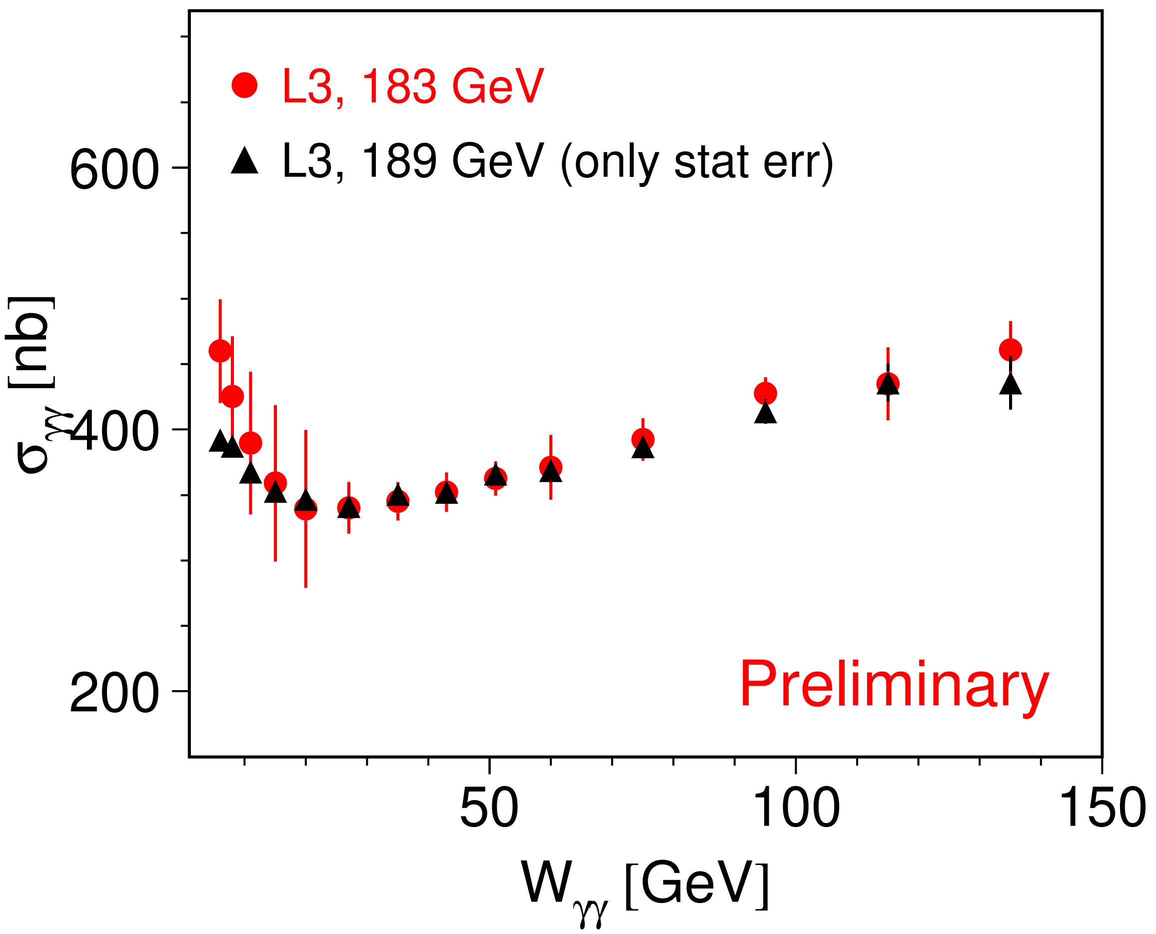

- At end of 1998, $\mathcal{L} \sim 150\ \mathrm{pb}^{-1}$
- The results at 183 GeV and 189 GeV are consistent !
- The statistical and experimental errors will be improved.
- An improvement of the MC generators is desirable !

Inclusive charged hadron production for $|\eta| < 1.5$

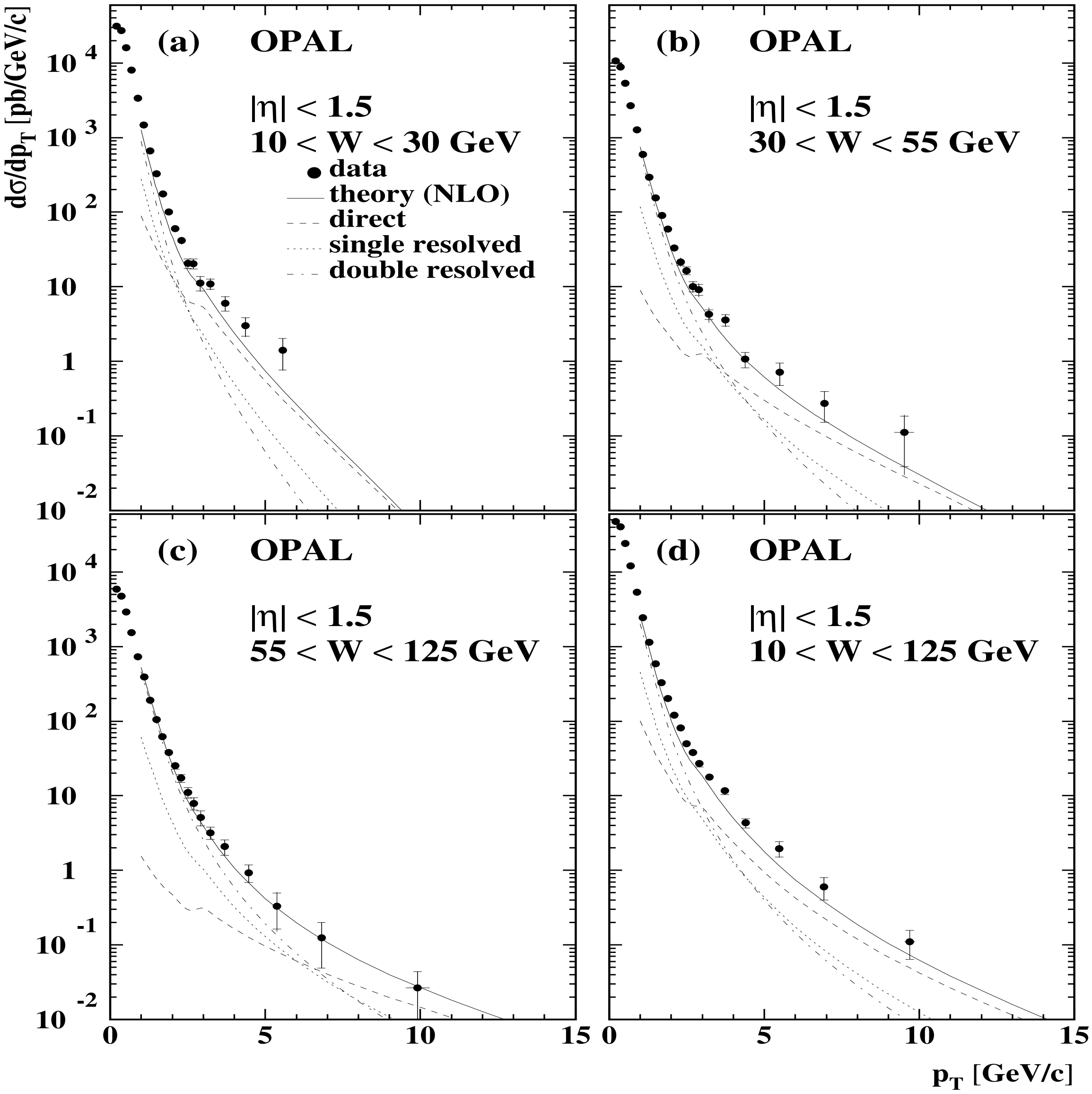

- NLO calculation by Binnewies, Kniehl and Kramer. (Phys. Rev. D53, 6110, 1996)
- The direct component is dominant at high p_T.
- For low $W_{\gamma\gamma}$, the NLO calculations lie below the data.
- For high $W_{\gamma\gamma}$, the agreement is good.

Inclusive particles $d\sigma/dp_T$

- Compare to γp and (π, K)p interactions.
- The γp and (π, K)p are normalised to the low p_T region.

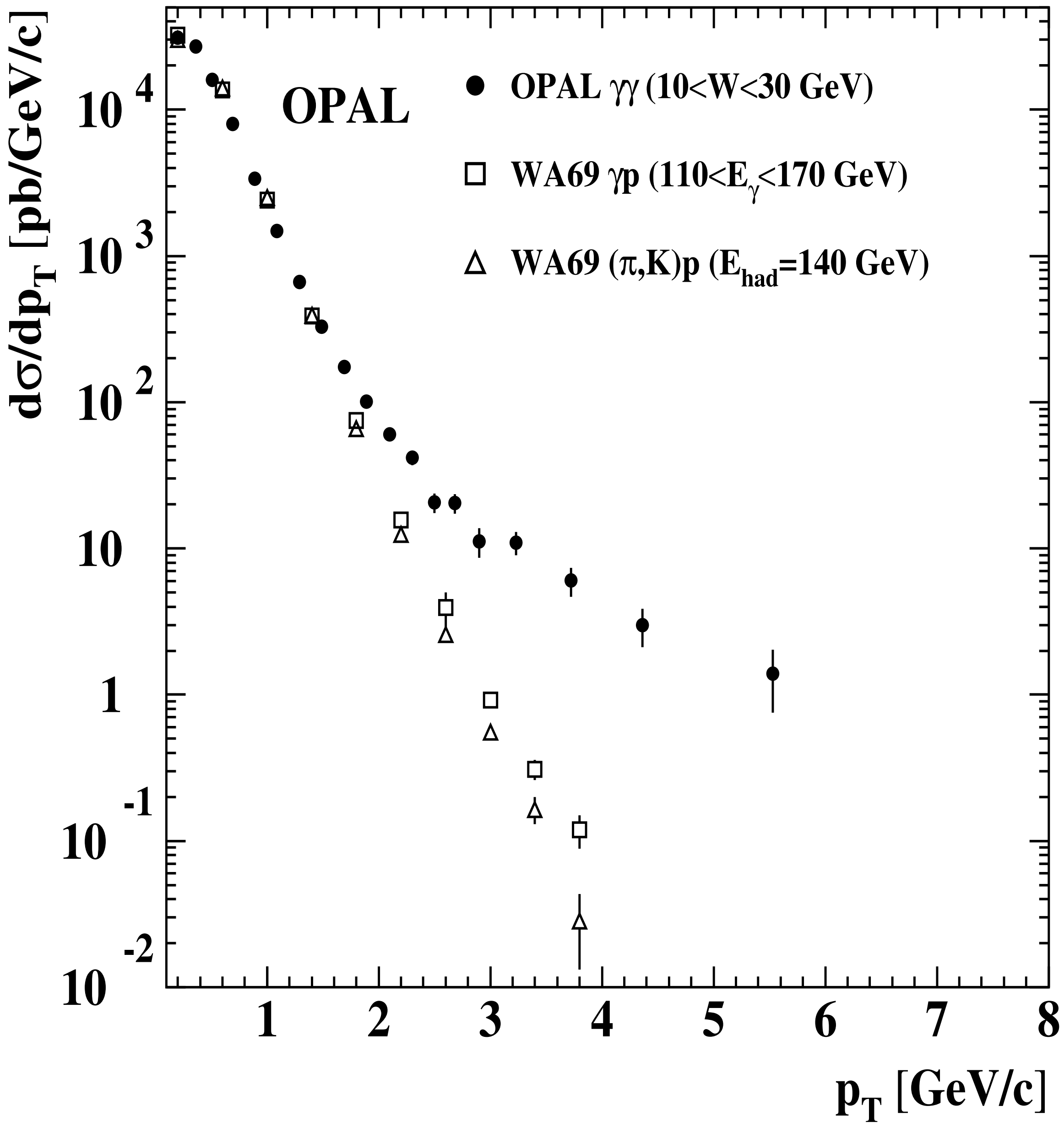

⇨ The $\gamma\gamma$ interaction is much harder because of the direct component.

Inclusive charged particle production $d\sigma/d\eta$ for $|p_T| > 1.5$ GeV

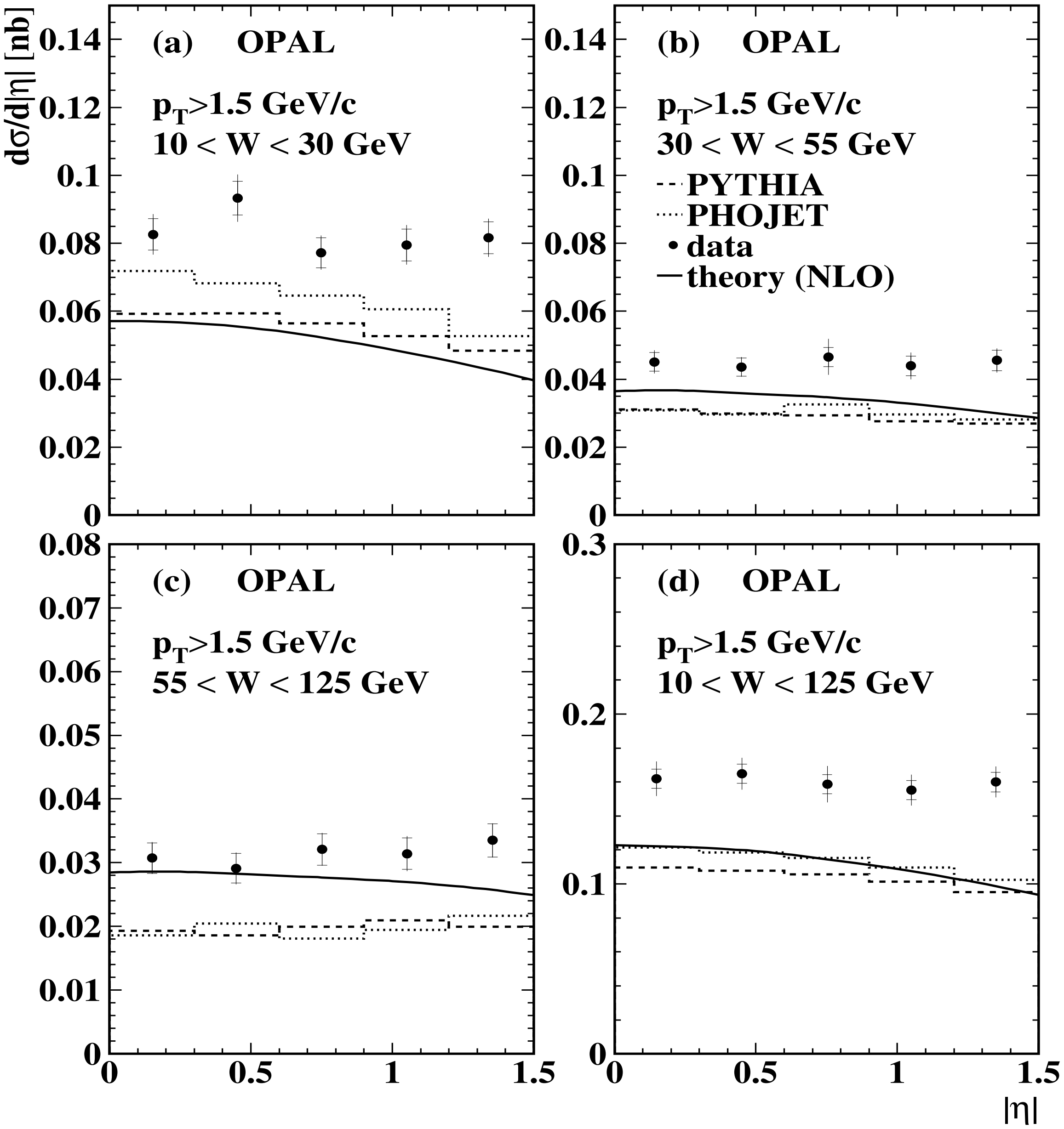

- ⇨ Monte Carlos and NLO calculation lie below the data for $W < 55$ GeV.
- ⇨ NLO calculation agrees better for 55 GeV $< W <$ 125 GeV.

$\rho^0 - \rho^0$ elastic scattering

$\gamma\gamma \to \rho^0\rho^0 \to \pi^+\pi^-\pi^+\pi^-$ at 183 GeV

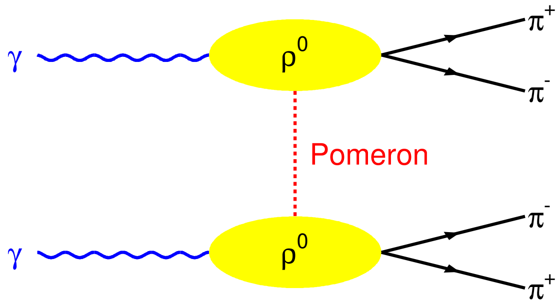

➜ The cross-section is expected to remain large at high $W_{\gamma\gamma}$ because of the Pomeron exchange.

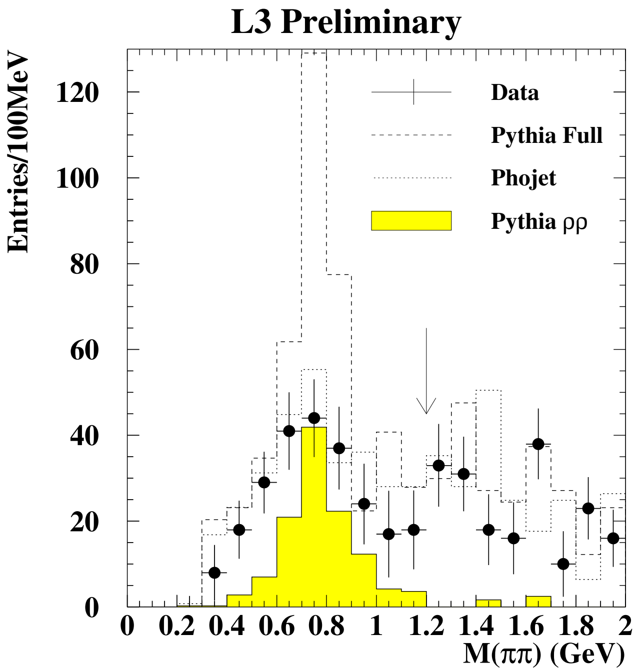

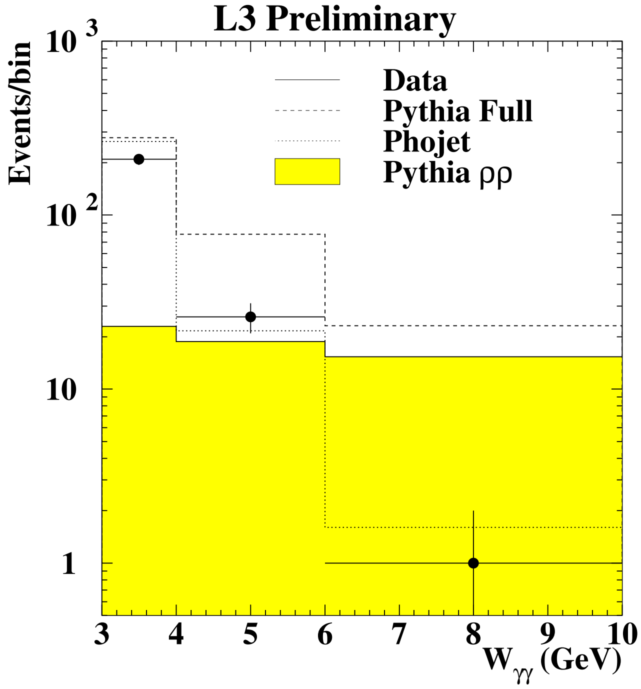

⇨ For $W_{\gamma\gamma} < 10$ GeV, the cross-section estimated by PYTHIA is too large.

⇨ The measurement for $W_{\gamma\gamma} > 10$ GeV is difficult, but important.

Inclusive Charm Production

❑ Motivation :

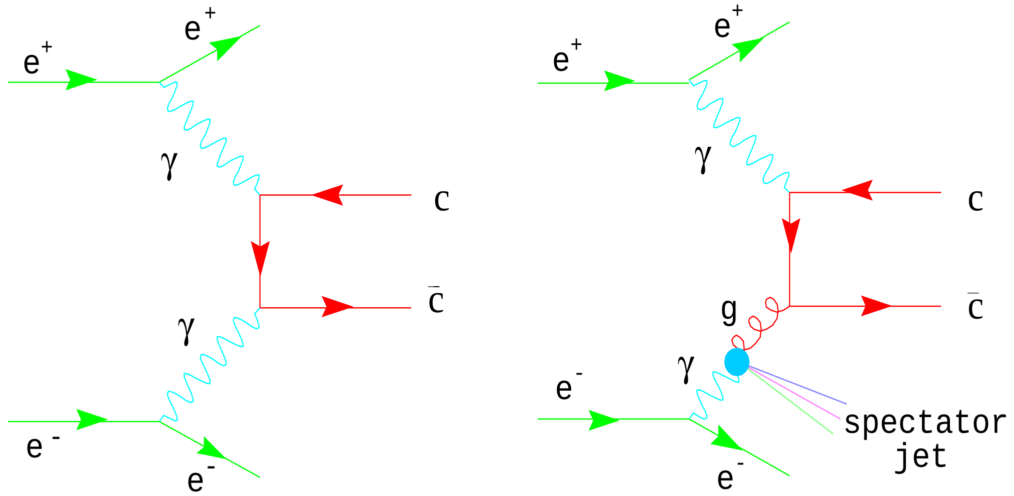

Direct   Single Resolved

➪ The cross-section is calculable by pQCD because of heavy m_c. ➜ good test of pQCD

➪ Provide information about gluon content of photon.

➪ Constrain mass of charm quark.

❑ Charm identification :

ALEPH : D^{*+} tag ($c \rightarrow D^{*+}X$)

L3 : lepton tag ($c \rightarrow l^{\pm}X$, $l^{\pm} \equiv e^{\pm}, \mu^{\pm}$)

D^{*+} tag (in progress)

❑ Data :

ALEPH : 91 GeV, $\mathcal{L} = 73\ \mathrm{pb}^{-1}$

L3 : 91 - 183 GeV, $\mathcal{L} = 165\ \mathrm{pb}^{-1}$

Inclusive Charm Production

Electron ID :

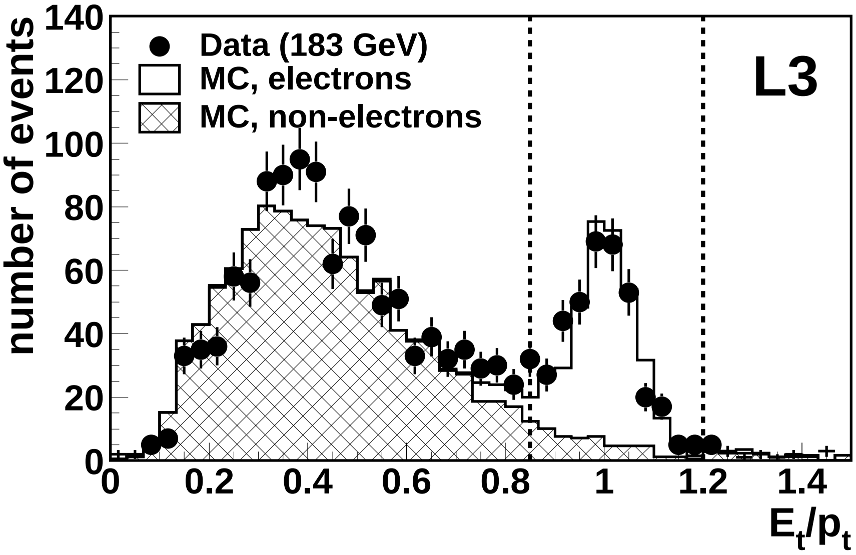

$D^{*\pm} \rightarrow D^0\pi_s^\pm \rightarrow K^\mp\pi^\pm\pi_s^\pm$

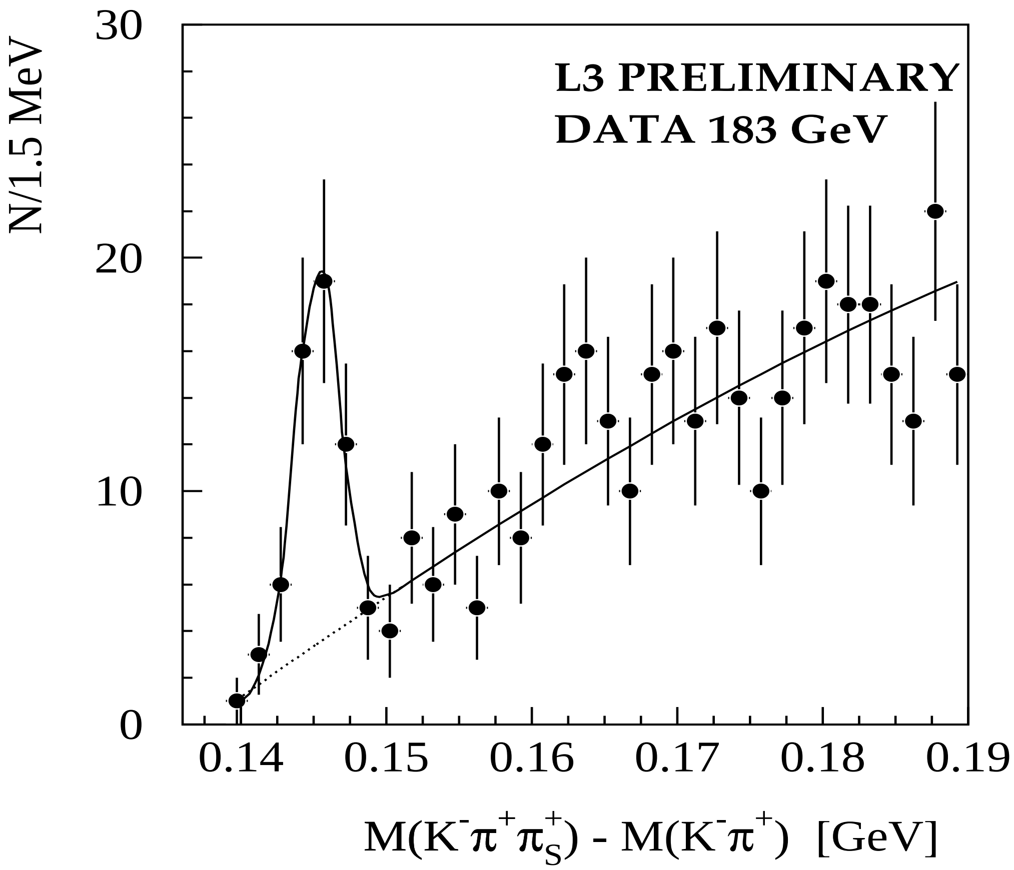

Inclusive Charm Production

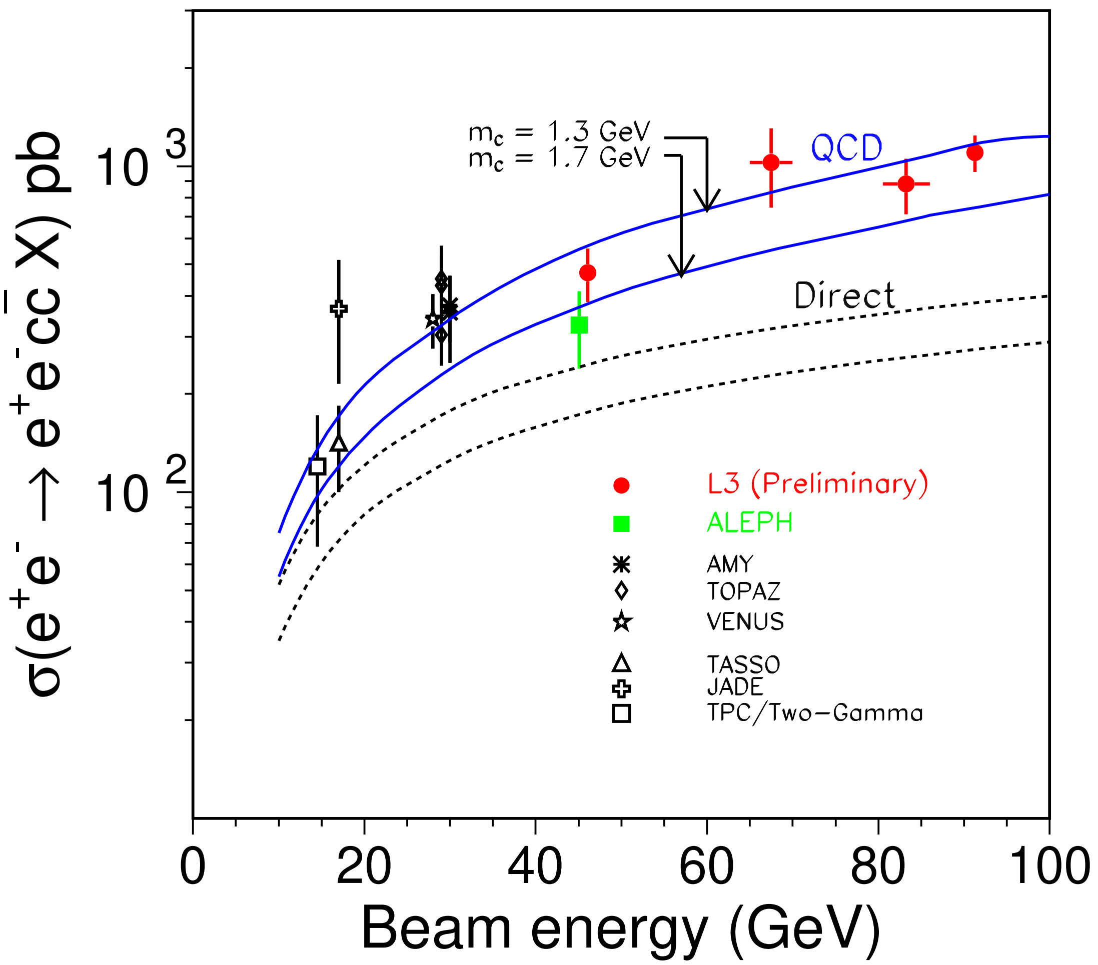

- QCD calculation by Drees, Krämer, Zunft and Zerwas. (Phys. Lett. B306, 371, 1993)
- $\sigma(e^+e^- \to e^+e^- c\bar{c}X)$ increases with the beam energy.
- The direct process is insufficient to describe the data. ➜ The resolved processes are necessary.

Photon Structure Function

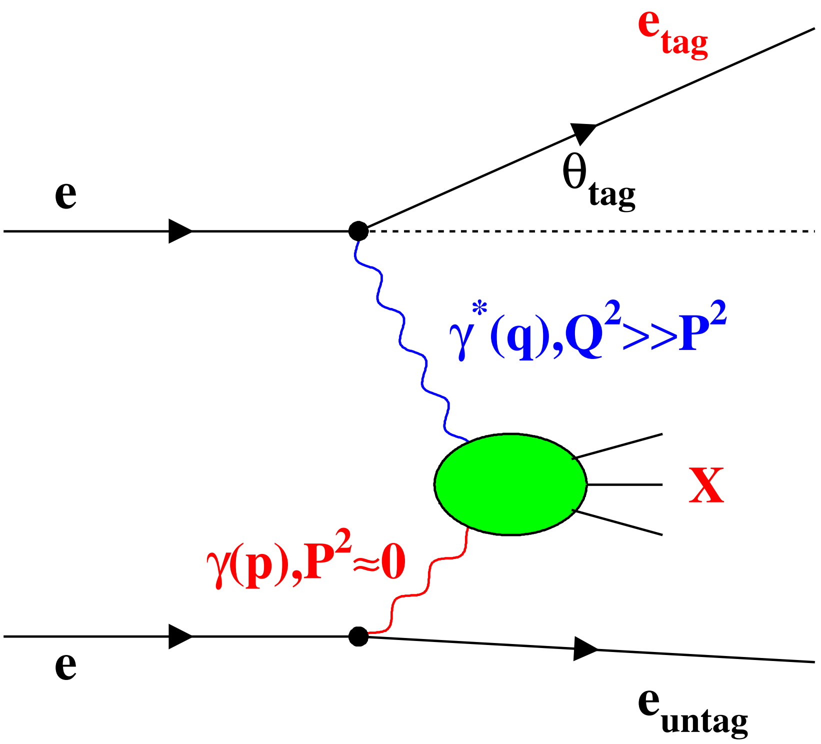

$$\frac{d^2\sigma_{e\gamma\to e\mathrm{X}}}{dx\,dQ^2} = \frac{2\pi\alpha^2}{xQ^4}[(1+(1-y)^2)F_2^\gamma(x,Q^2) - y^2 F_L^\gamma(x,Q^2)]$$

$$x = \frac{Q^2}{Q^2+P^2+W_{\gamma\gamma}^2}\ ,\ y = 1 - \frac{E_{tag}}{E_{beam}}\cos^2\frac{\theta_{tag}}{2} << 1$$

- ⇨ Only F_2^γ is measurable since y^2 is small.
- ⇨ The effect of longitudinal photons can be seen in the azimuthal correlations of $e\gamma \longrightarrow el^+l^-$.

F_2^γ : Physics

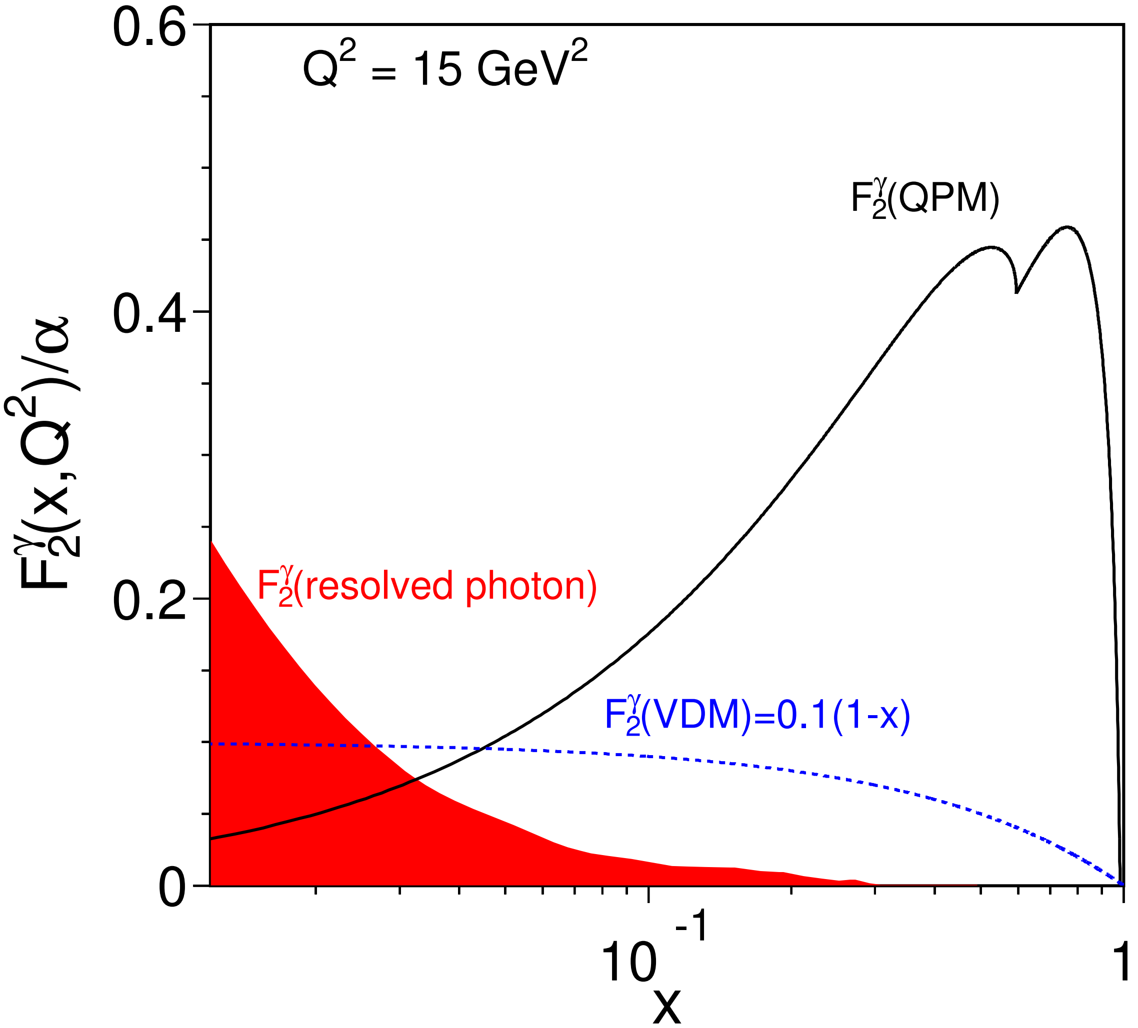

- **At high x ➜ Quark constituents are dominant.**
- **At low x ➜ Gluon constituents are dominant.**

➪ **The low x region is sensitive to the gluon density.**

F_2^γ : Kinematic region

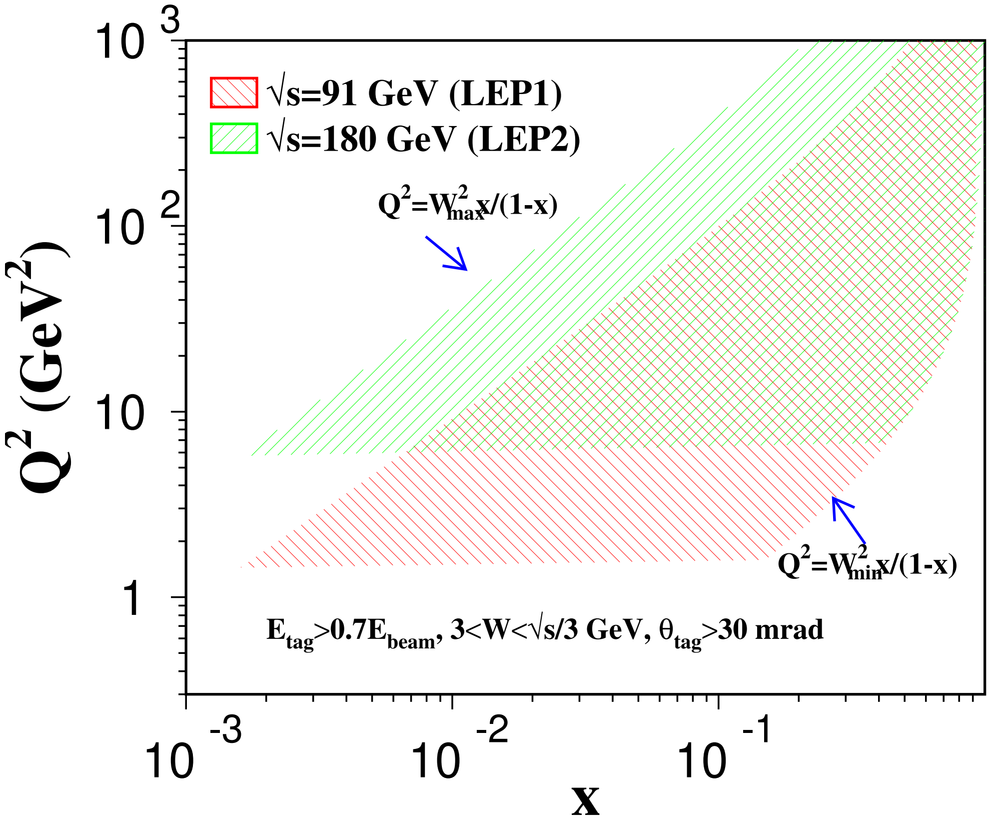

Exp	detector	Q^2 (LEP1)	Q^2 (LEP2)
L3	Lumi Cal.	1.2 - 9.0	9 - 30 $(\sqrt{s} \simeq 183$ GeV)
	Endcap	40 - 500	
OPAL	SW Cal.	1.5 - 6.0	6 - 20 $(\sqrt{s} \simeq 161 - 172$ GeV)
	Forward	6 - 30	20 - 100
	Endcap	60 - 400	
ALEPH	Lumi Cal.	4 - 30	
	ECAL	50 - 2400	
DELPHI	SAT	4 - 30	

- The Q^2 ranges from 1 GeV^2 to 2400 GeV^2.
- The x ranges from 0.002 at low Q^2 to $\sim$ 1 at high Q^2.

F_2^γ : Monte Carlo

1. Monte Carlo Programs :

- $F^{\gamma}_{2,\mathrm{QCD}}$, $e^+e^- \to e^+e^-$hadrons :
  1. TWOGAM, Nova, Olshevski and Todorov (DELPHI)
  2. PHOJET, Engel and Ranft
  3. HERWIG, Marchesini et al.
  4. PYTHIA, Sjöstrand and Schuler

- $F^{\gamma}_{2,\mathrm{QED}}$, $e^+e^- \to e^+e^-\mu^+\mu^-$:
  1. JAMVG, Vermaseren
  2. DIAG36, Berends, Daverveldt and Kleiss
  3. RADCOR, Berends, Daverveldt and Kleiss

2. $F^{\gamma}_{2,\mathrm{QCD}}$ parametrisation :

- GRV-LO/HO, Glück, Reya and Vogt (1992)
  evolution starts at a low value of Q_0^2 ($= 0.25$ GeV^2)
- SaS-1d, Schuler and Sjöstrand (1995, 1996)
  evolution starts at a low value of Q_0^2 ($= 0.36$ GeV^2)
- LAC, Abramovicz, Charchula and Levy (1991)
  evolution starts at a high value of Q_0^2 ($= 4$ GeV^2)

⇨ The effect of $P^2 \neq 0$ is not taken into account, which would reduce the predictions.

$F_{2,\mathrm{QCD}}^{\gamma}$: MC comparison

❑ **Compare to the L3 data :**

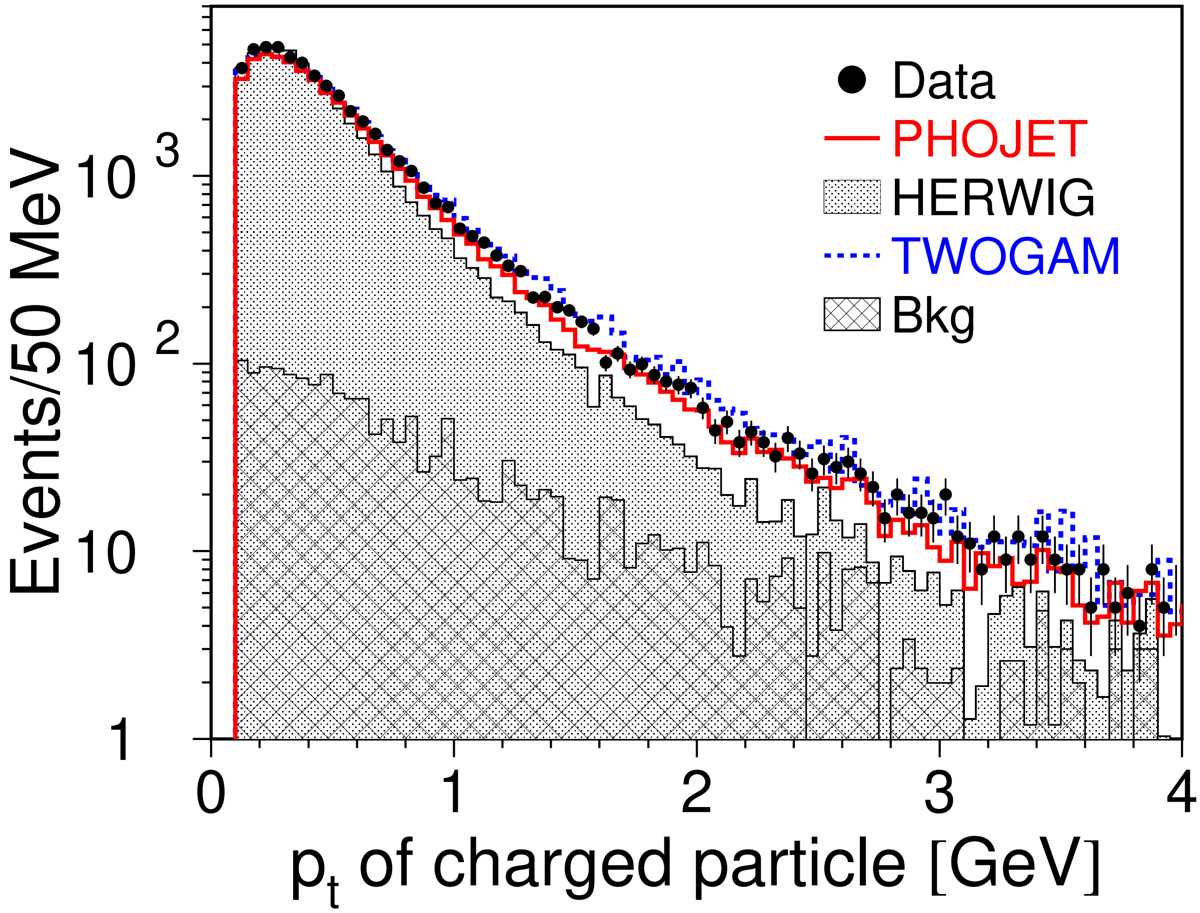

⇨ **PHOJET and TWOGAM describe the data better than HERWIG.**

$F_{2,QCD}^{\gamma}$: L3 Energy Flow

❑ Compare to the L3 data :

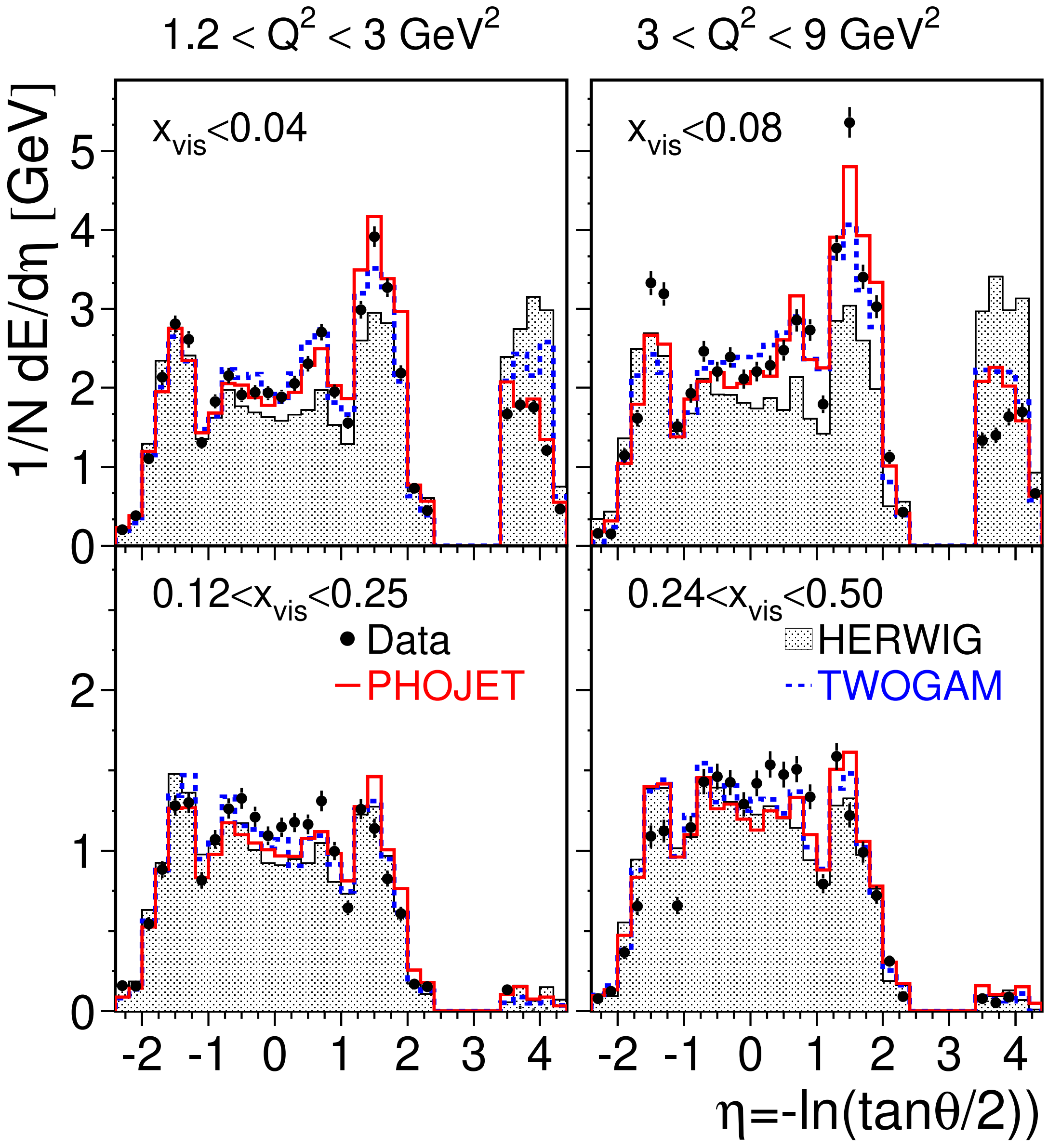

❑ Again, PHOJET and TWOGAM do better than HERWIG.

❑ HERWIG agrees better at high x.

$F_{2,\mathrm{QCD}}^{\gamma}$: OPAL Energy Flow

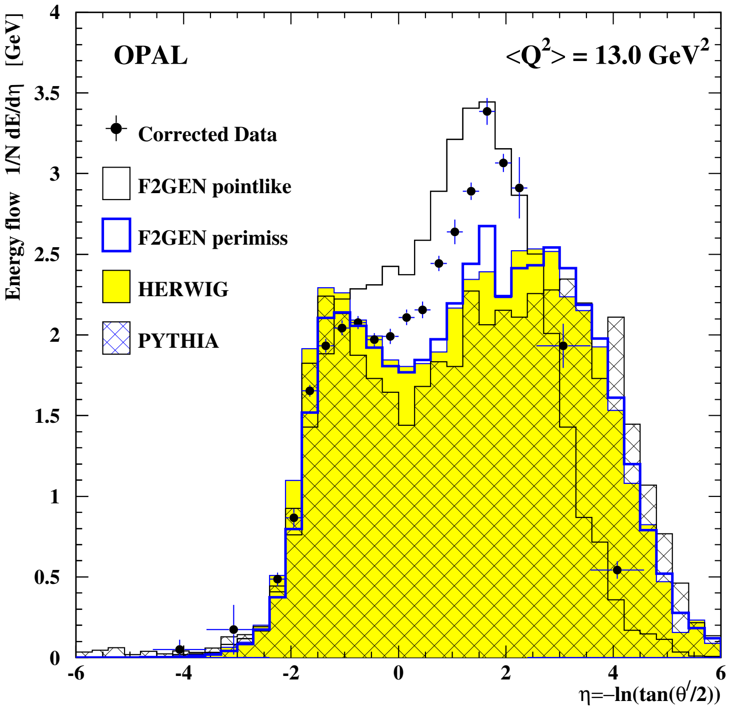

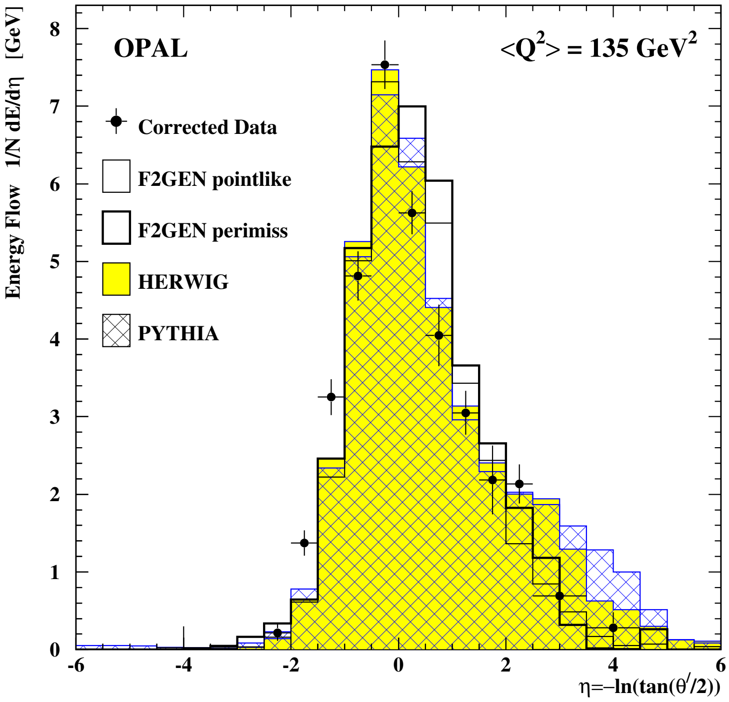

⇨ Agreement is better at high Q^2.

W_{vis} Measurement

- Due to detector acceptance and efficiency

  ⇨ $W_{vis} < W_{\gamma\gamma}$ ➔ Unfolding

- Improve W_{vis} ➔ Use kinematics of e_{tag}

$$W_{rec}^2 \equiv (p_+^{e_{in}} - p_+^{e_{tag}})(\sum_i p_-^i) - |p_t^{e_{tag}}|^2$$

$$p_\pm \equiv E \pm p_z$$

* Physics at LEP2, CERN 96-01, Vol.2, 201.

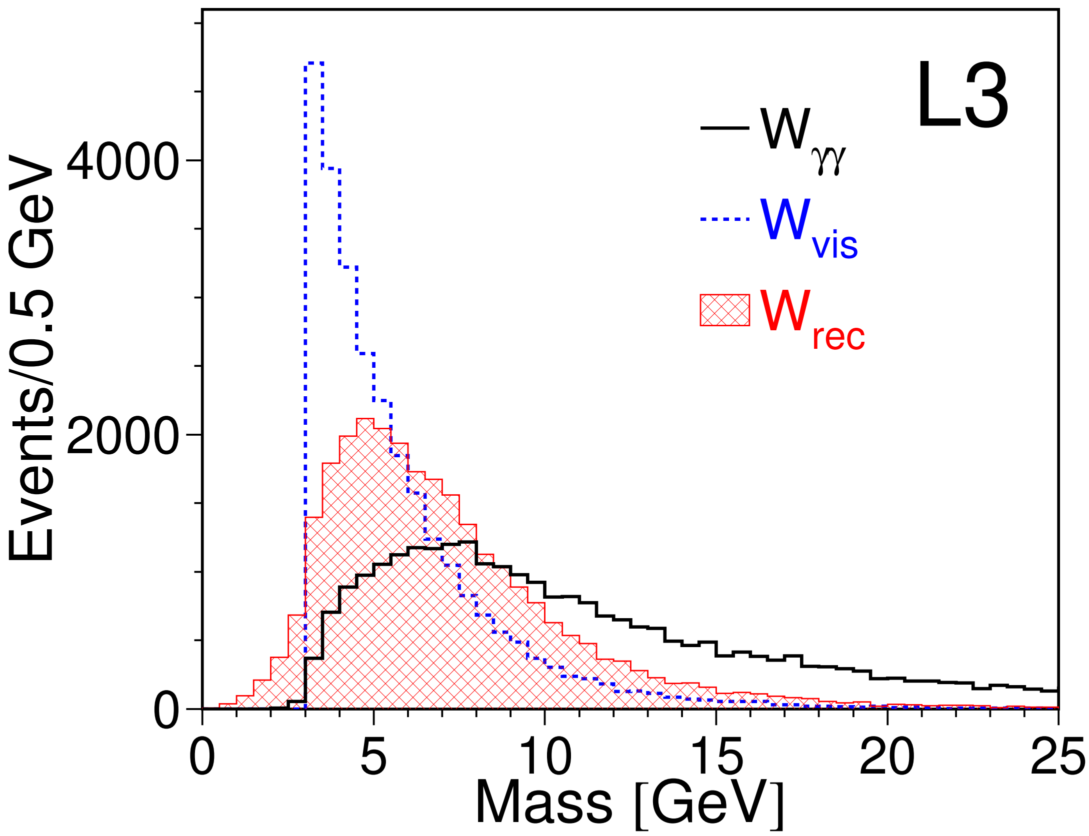

- Use Unfolding for x_{rec} ➔ x.

- Extract F_2^γ from differential cross-section.

$F_{2,\mathrm{QCD}}^{\gamma}$: Modelling Dependence

- Unfold the data with different Monte Carlos. ($\sqrt{s} \simeq 91$ GeV)
- The OPAL results are obtained with HERWIG.

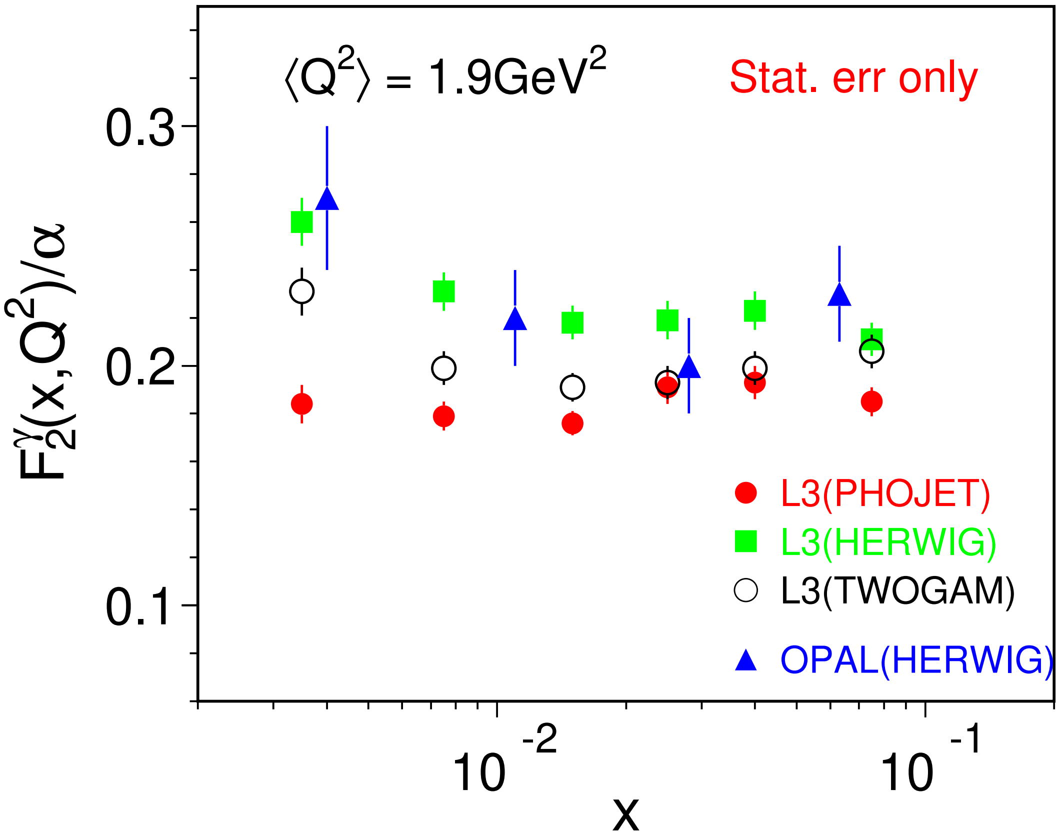

⇨ L3 and OPAL agree if they use the same MC, but HERWIG doesn't describe the data as well as PHOJET.

⇨ The discrepancy is much larger at low x.

$F^{\gamma}_{2,\mathrm{QCD}}$: low Q^2

❑ **The measured $F^{\gamma}_{2,\mathrm{QCD}}$ at low Q^2 ➜ access to low x.**

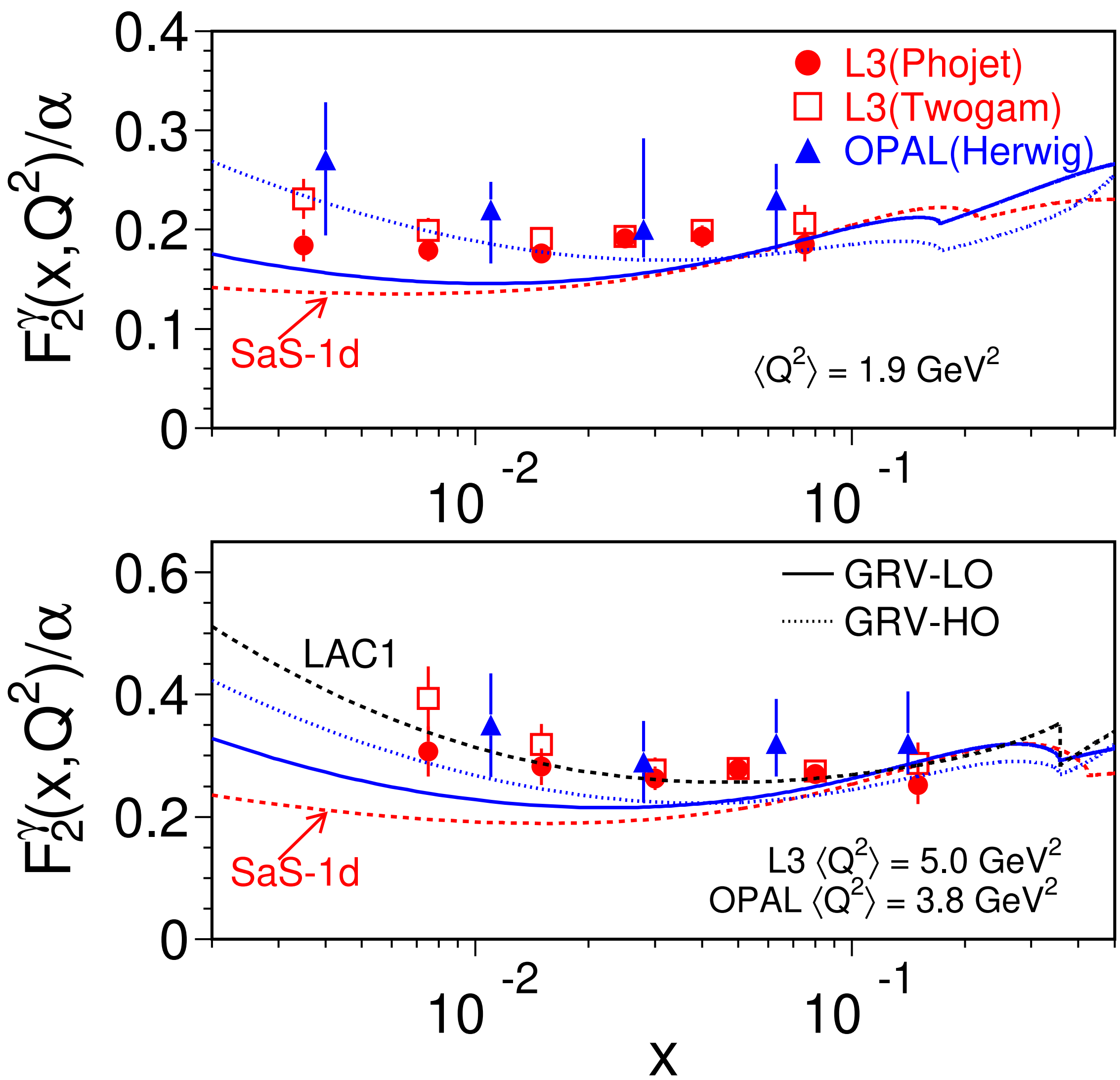

⇨ **GRV-HO describes the low x better than GRV-LO.**

⇨ **LAC1 agrees with the data at $Q^2 = 5\ \mathrm{GeV}^2$ apparently.**
➜ disagree with the high Q^2 data and Q^2 evolution.

⇨ **F^{γ}_2 does not decrease at low x.**

$F_{2,\mathrm{QCD}}^{\gamma}$: medium Q^2

❑ The measured $F_{2,\mathrm{QCD}}^{\gamma}$ at medium Q^2

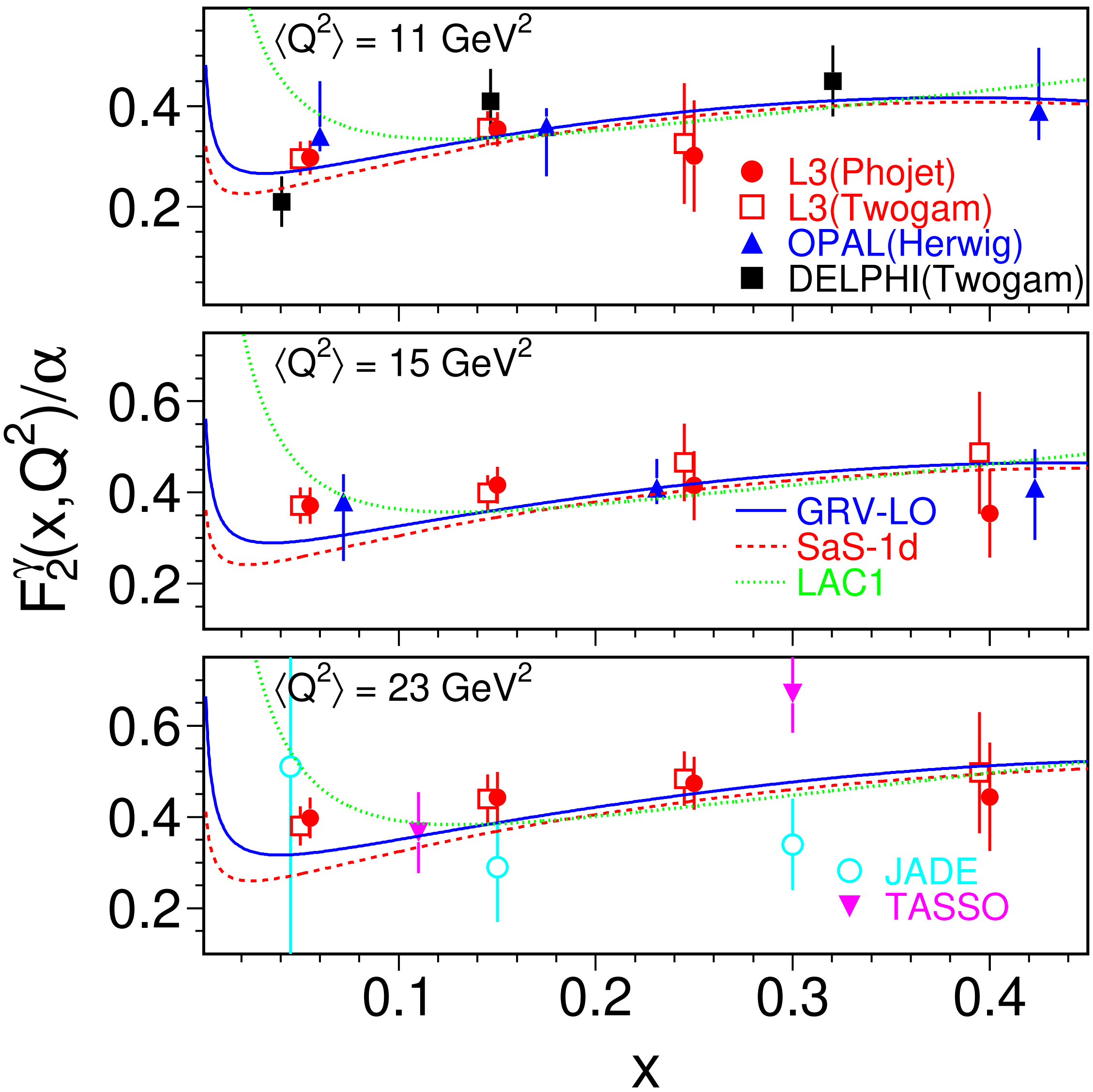

➩ The modelling dependence is improved at high Q^2.

➩ $x > 0.1$, the agreement is good.

➩ $x < 0.1$, the data lie between LAC1 and GRV-LO.

➩ LEP has much improved the measurement of F_2^{γ} with respect to PETRA.

$F^{\gamma}_{2,\mathrm{QCD}}$: high Q^2

- The measured $F^{\gamma}_{2,\mathrm{QCD}}$ at high Q^2

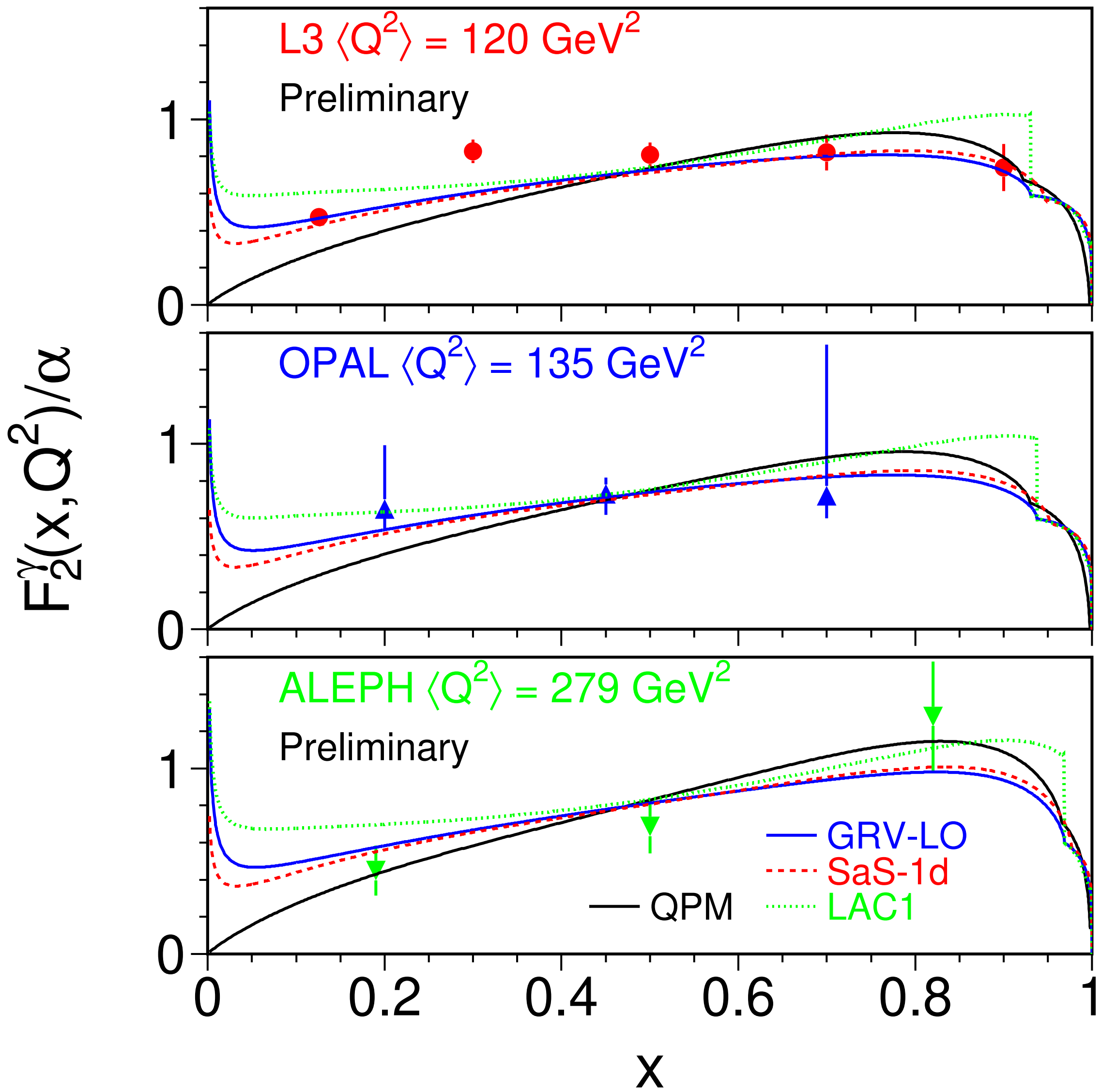

➩ QPM uses $m_u = m_d = 0.325$ GeV, $m_s = 0.5$ GeV, $m_c = 1.6$ GeV

➩ The QPM model is insufficient to describe the data for $x < 0.3$. (OPAL and L3) ➜ need the resolved processes.

➩ GRV-LO and SaS-1d agree with the data well at high Q^2.

$F_{2,\mathrm{QCD}}^{\gamma}$: Q^2 evolution

❑ The measured F_2^γ as a function of $\ln Q^2$

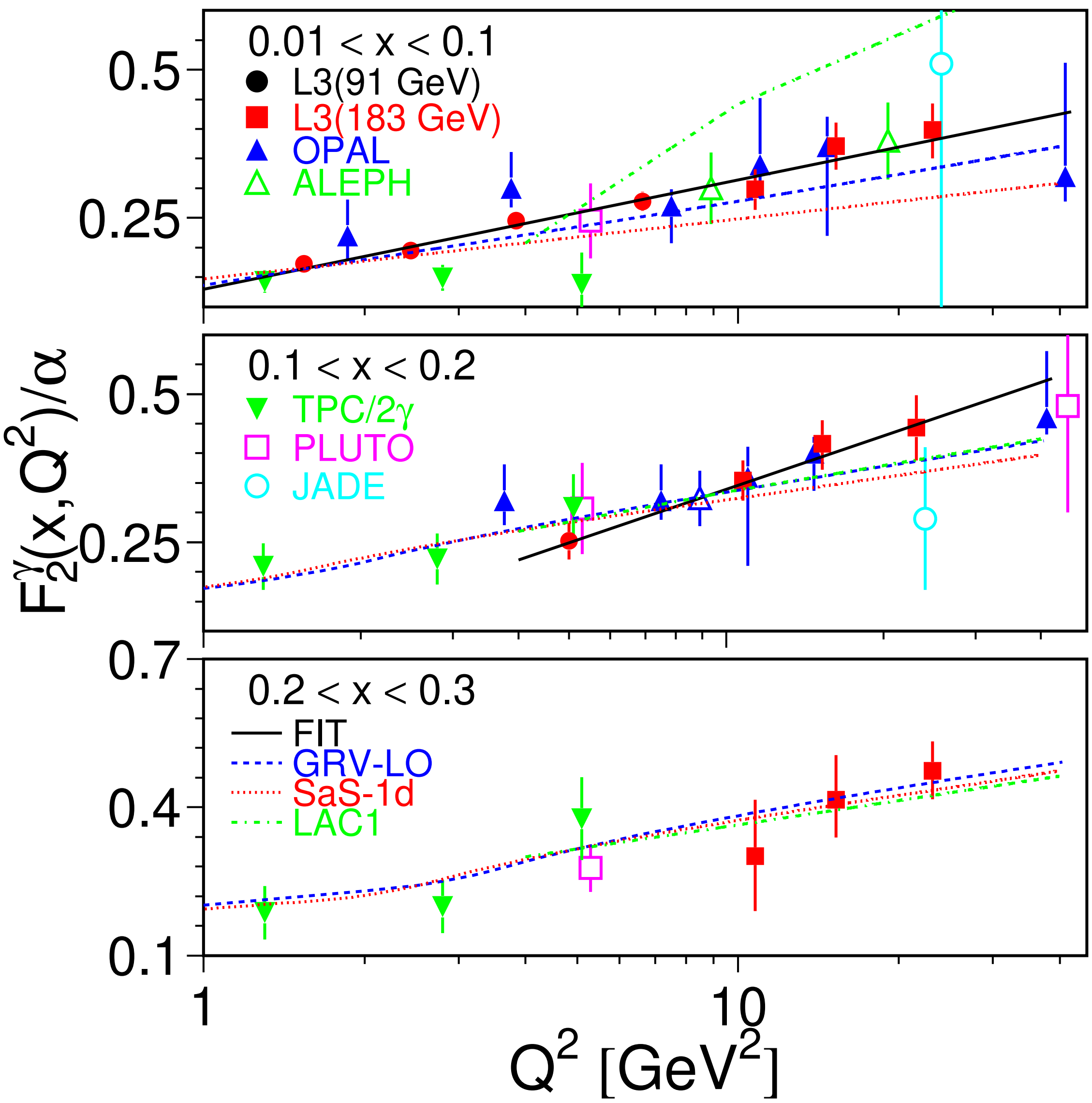

⇨ Agree with $\ln Q^2$ evolution.

⇨ At low x, LAC1 increases too fast and SaS-1d too slowly. At high x, the agreement is reasonable.

$F_{2,\mathrm{QCD}}^{\gamma}$: Q^2 evolution

❑ **The measured F_2^{γ} as a function of $\ln Q^2$ at high x.**

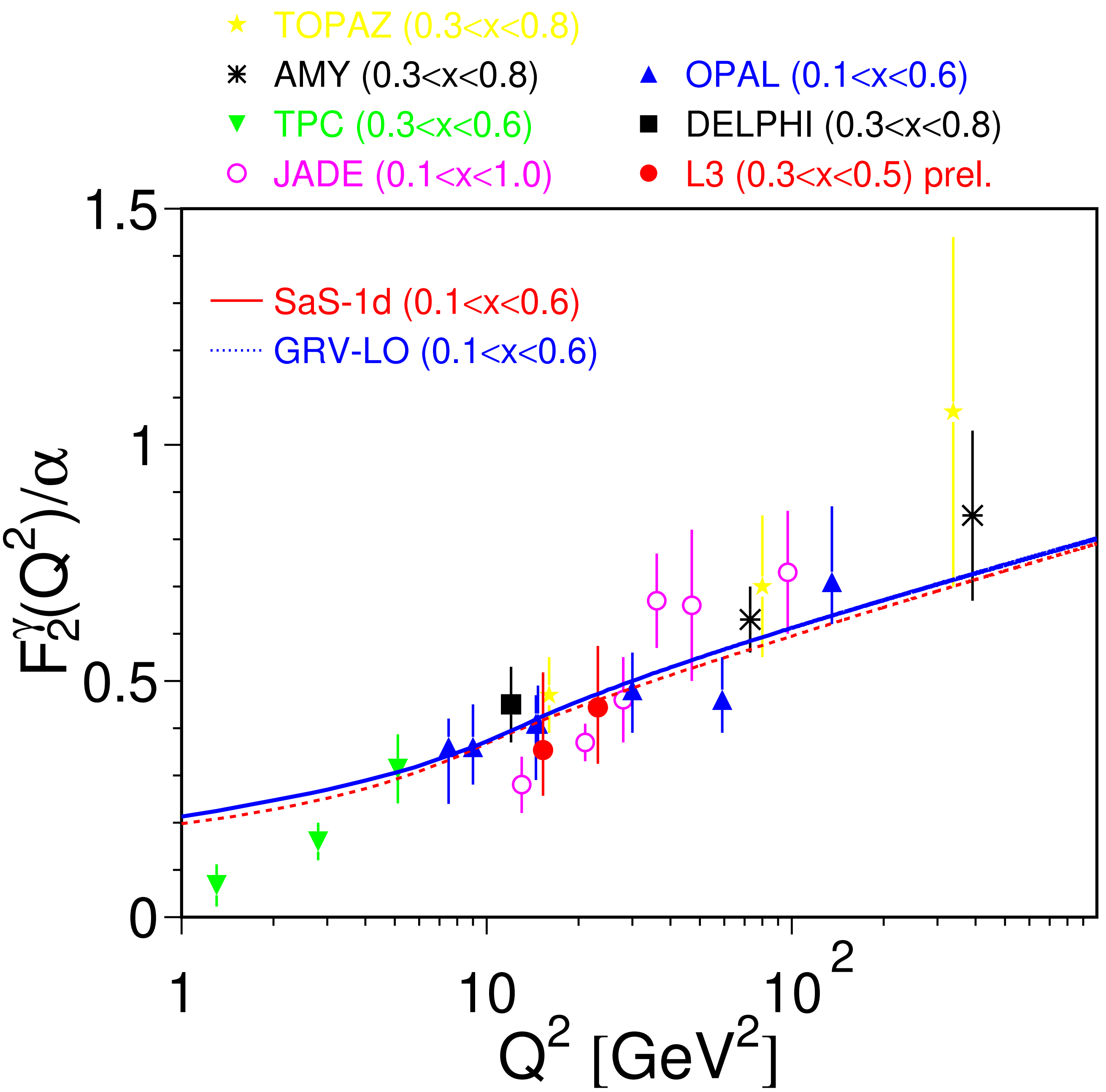

⇨ **Agree with $\ln Q^2$ evolution.**

$F_{2,\mathrm{QED}}^{\gamma}$: x Dependence

❑ The $F_{2,\mathrm{QED}}^{\gamma}$ is measured at $\mu^+\mu^-$ final state.

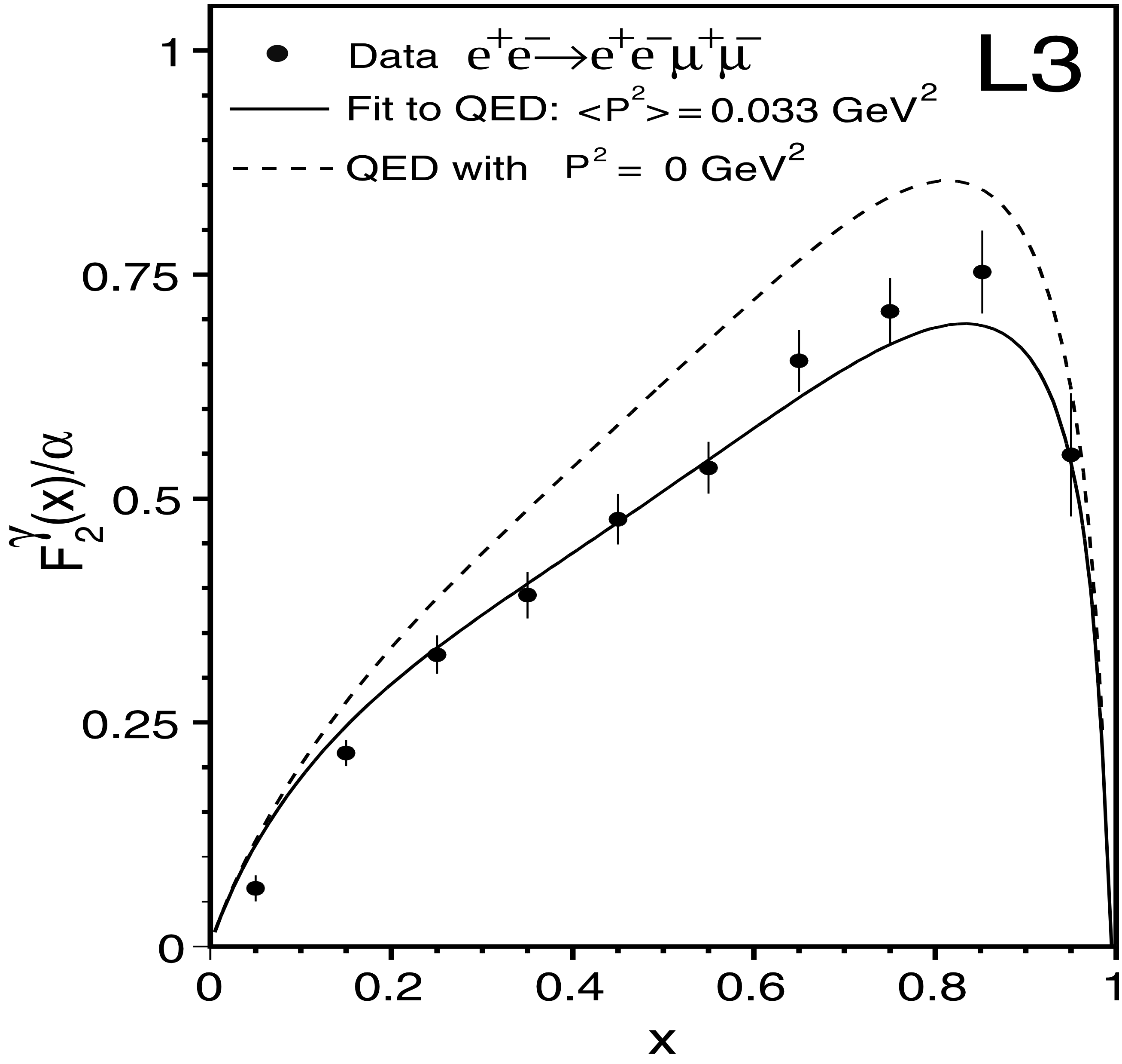

➩ Consistent with QED prediction with non-zero photon virtuality.

➩ $\langle P^2 \rangle = 0.033 \pm 0.005$ GeV^2 agrees with MC including Radiative Corrections on the incoming and outgoing electrons. (*Nucl. Phys. B253, 421, 1985)

➩ $\langle P^2 \rangle = 0.024$ GeV^2 predicted by MC without R.C.

Azimuthal Correlations

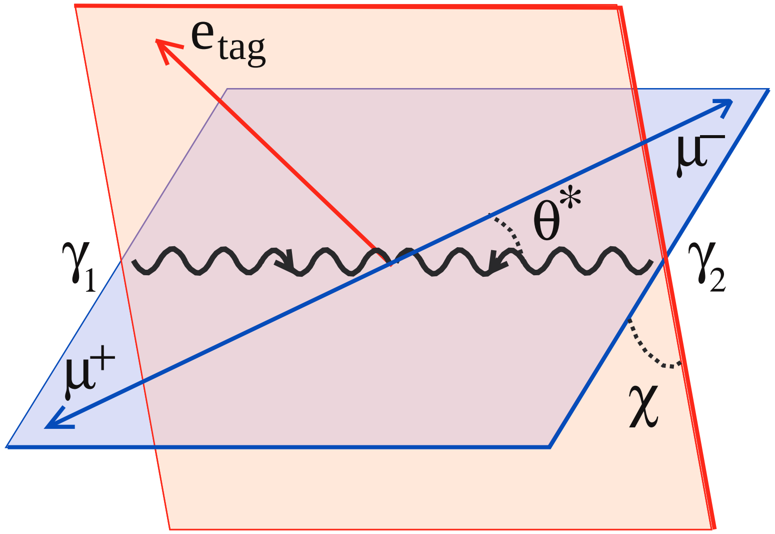

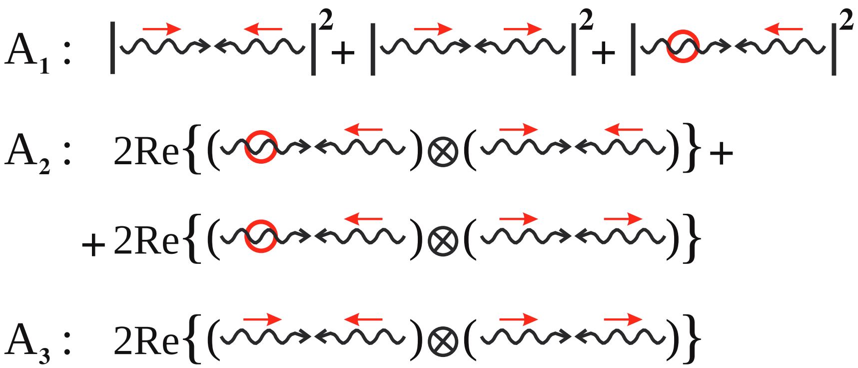

$$\frac{d^4\sigma}{dx\,dy\,dz\,d\chi} = \frac{2\pi\alpha^2}{Q^2}\frac{1+(1-y)^2}{xy}\left[A_1(x,z) + A_2(x,z)\cos\chi + A_3(x,z)\cos 2\chi\right]$$

$$z = \cos\theta^*$$

$A_1 \propto F_2^\gamma \Rightarrow$ **Sum of all photon helicity states**

$A_2 \propto F_A^\gamma \Rightarrow$ **Interference of longitudinal-transverse photons**

$A_3 \propto F_B^\gamma \Rightarrow$ **Interference of two transverse photons**

N.B. 'transverse' photons have helicity ± 1,
'longitudinal' photons have helicity 0.

F_A^γ and F_B^γ

❑ F_A and F_B measurement at L3

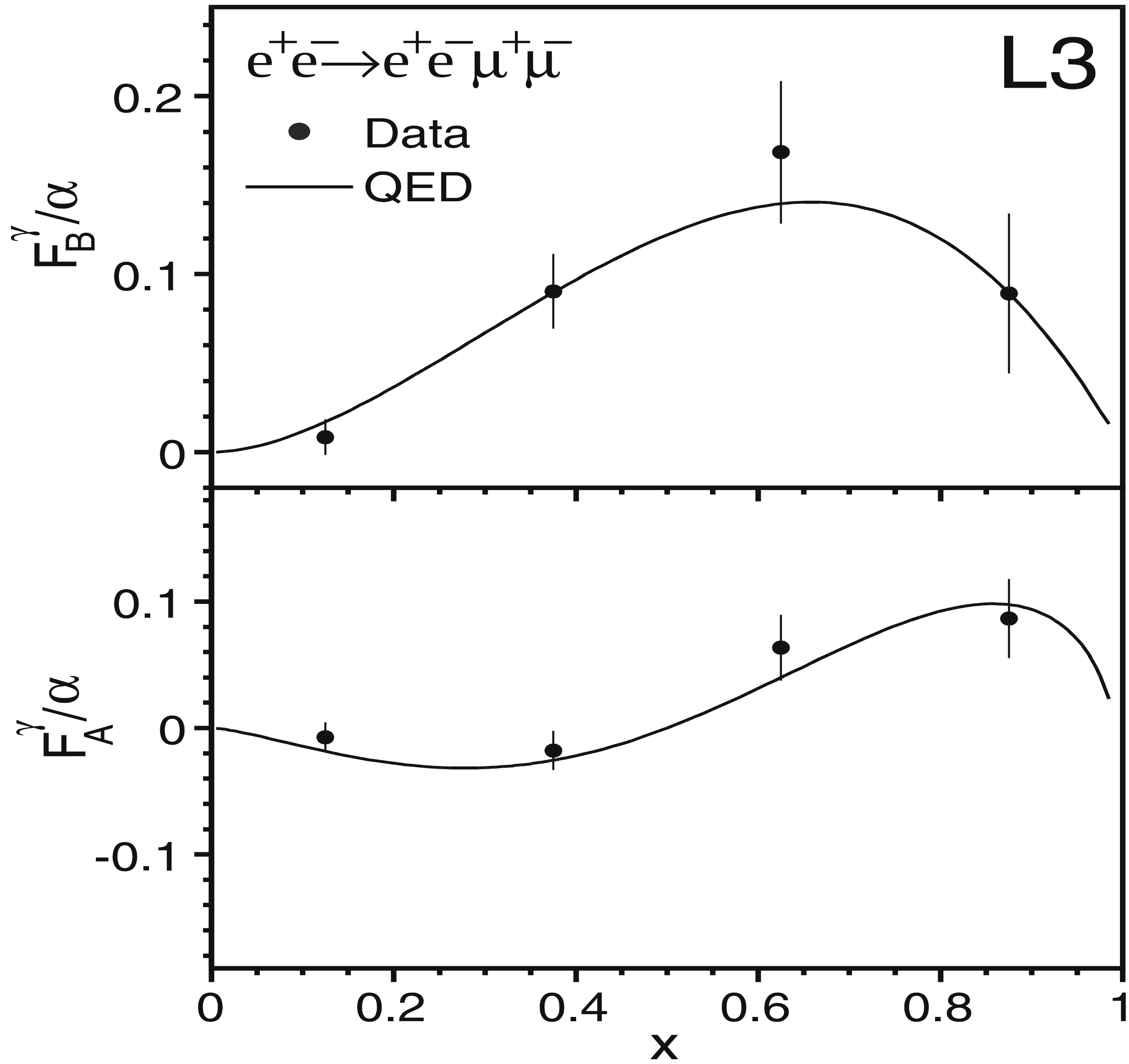

⇨ Non-zero F_A^γ is seen → $F_L^\gamma \neq 0$

⇨ Consistent with QED prediction.

F_A^γ and F_B^γ

❑ F_A/F_2^γ and F_B/F_2^γ measurement at OPAL

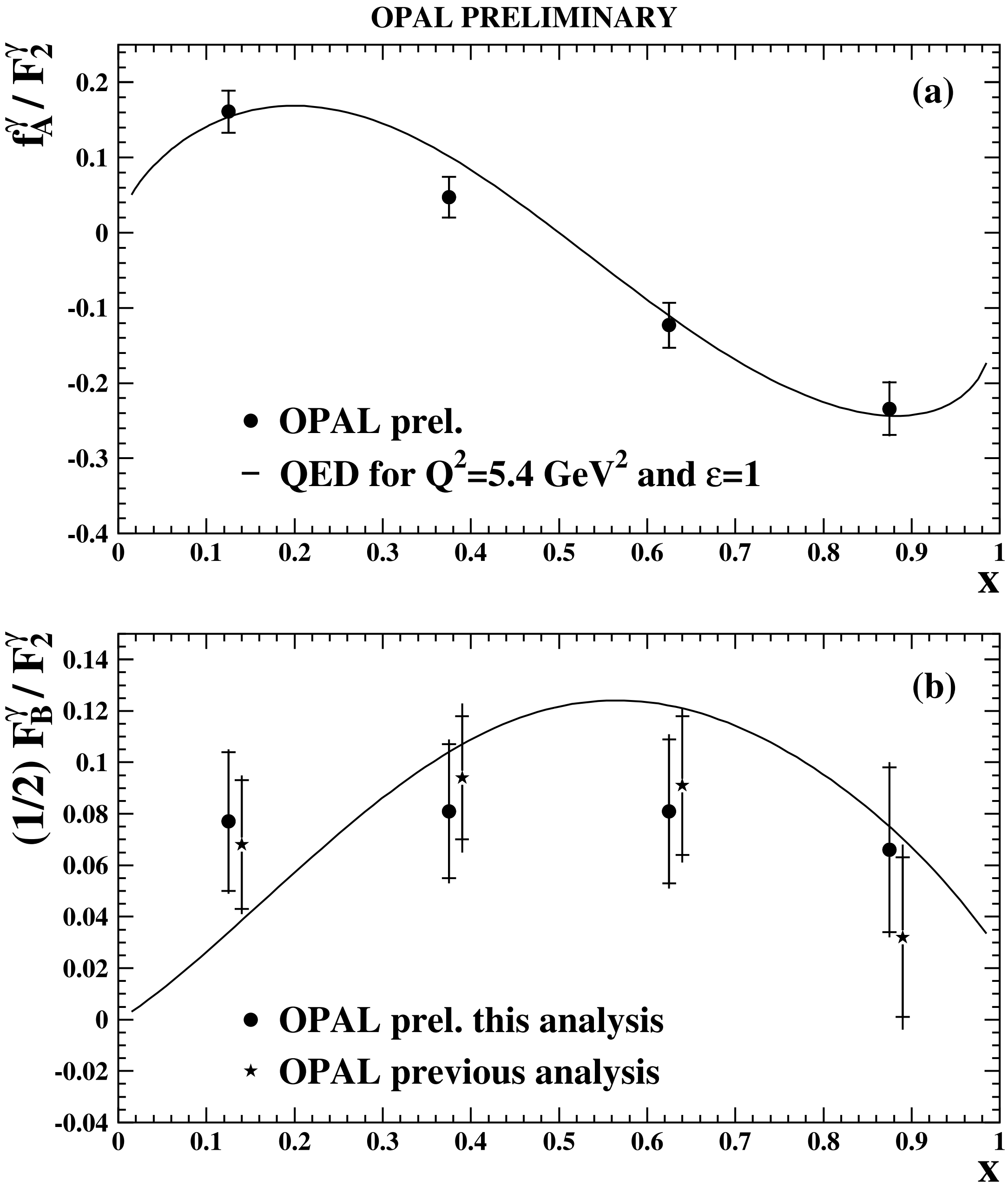

⇨ Good agreement with QED prediction.

$\sigma_{\gamma^*\gamma^*}$ (Double-tagged events)

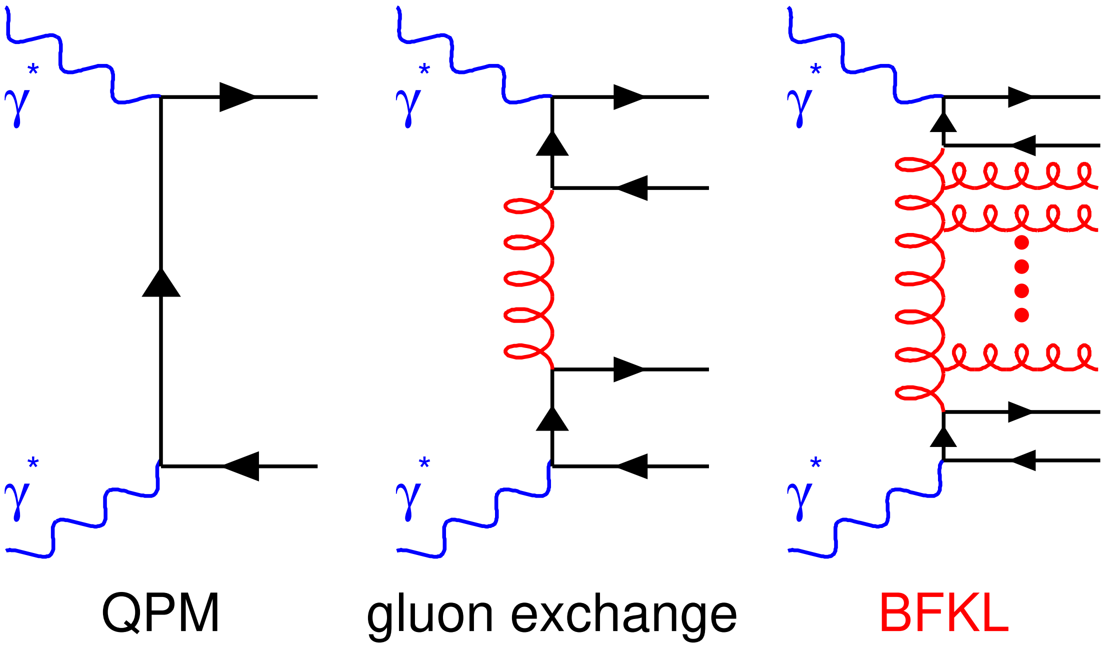

- J. Bartels et al. (Phys. lett. B389 742, 1996) and S.J. Brodsky et al. (Phys. Rev. D56 6957, 1997) point out the BFKL Pomeron can be investigated in $\gamma^*\gamma^*$ collisions.
  - ➩ BFKL diagram is dominant at high Q^2 and high $W_{\gamma^*\gamma^*}$.
  - ➩ two virtual photons ➜ double-tagged events

- In Leading order approximation :

$$\sigma_{\gamma^*\gamma^*} = \sigma_0 \left(\frac{s}{s_0}\right)^{\alpha_P - 1} \simeq \sigma_0 \left(\frac{W^2_{\gamma^*\gamma^*}}{\sqrt{Q_1^2 Q_2^2}}\right)^{\alpha_P - 1}$$

$$s_0 = \frac{\sqrt{Q_1^2 Q_2^2}}{y_1 y_2}$$

$$\alpha_P - 1 = 4 \ln 2 \frac{N_c \alpha_s}{\pi}$$

- Using $N_c = 3$, $\alpha_s = 0.2$ ➜ $\alpha_P - 1 \simeq 0.53 > 0.079$

- The measurement of $\sigma(e^+e^- \to e^+e^-\gamma^*\gamma^* \to e^+e^- + hadrons)$ is an excellent test for the BFKL Pomeron.

$\sigma_{\gamma^*\gamma^*}$: Analysis

- Data :
  L3 : 91 GeV, 140. pb^{-1}
  183 GeV, 51.9 pb^{-1}

- Monte Carlo :

  PHOJET: Engel and Ranft.
  (Phys. Rev. D54, 4246, 1995)

  TWOGAM: Nova, Olshevski and Todorov
  (Delphi Note 90-35)

  → Good agreement with single-tagged events
  → Neither of MCs use the assumption of BFKL Pomeron

- Event Selection :

  - The tagged electron is identified by :
    $E_{tag} > 30$ GeV for $\sqrt{s} \simeq 91$ GeV
    $E_{tag} > 40$ GeV for $\sqrt{s} \simeq 183$ GeV
    30 mrad $< \theta_{tag} <$ 66 mrad
  - The number of tracks > 2
  - $W_{vis} > 2$ GeV
  - $2 < \ln(s/s_0) < 6$

$\sigma_{\gamma^*\gamma^*}$: MC comparison

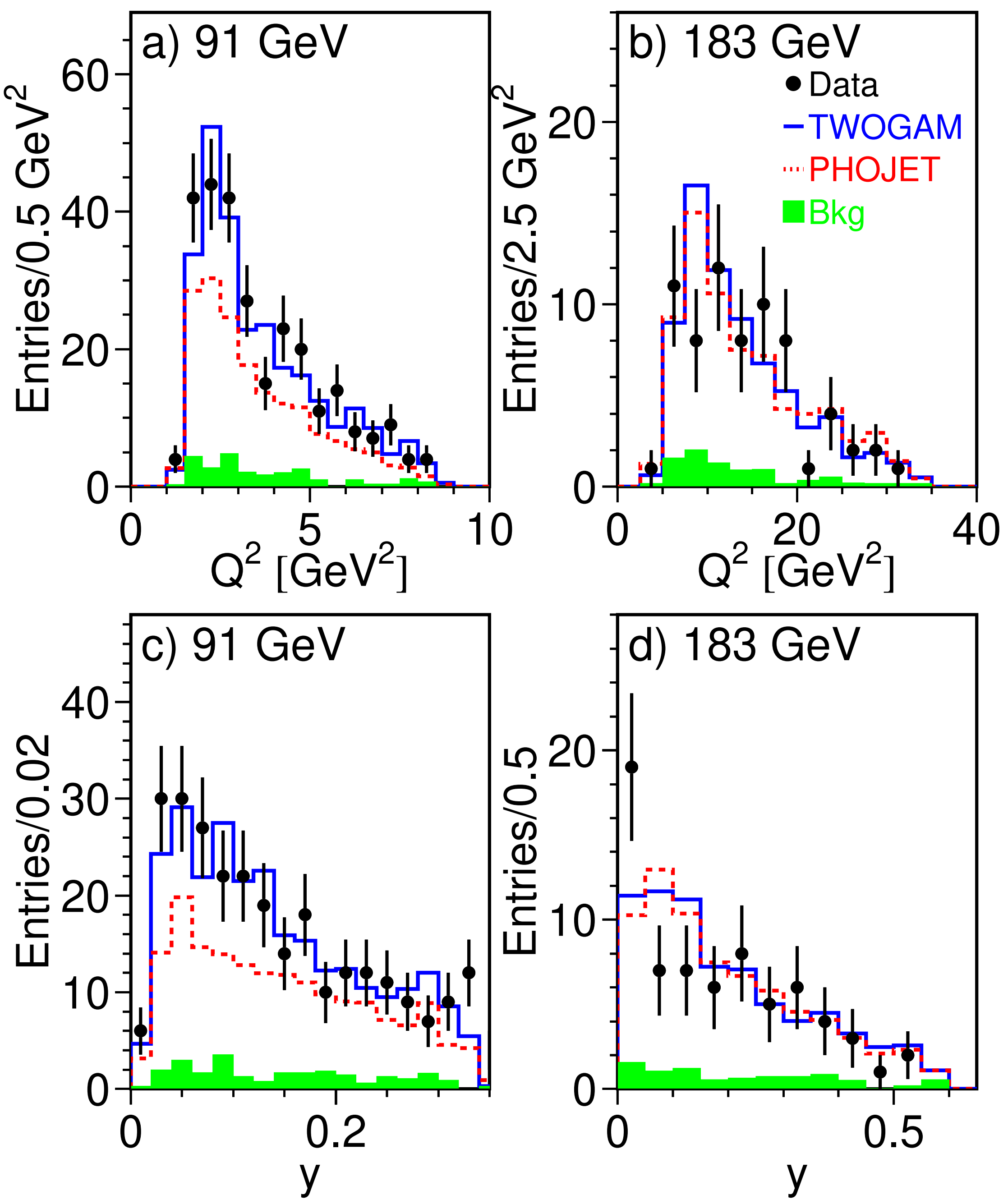

*Two entries per event

- **PHOJET** is a factor of **two lower** than the data at **91 GeV**.
- The backgrounds come from $e^+e^- \to e^+e^-\tau^+\tau^-$ and single tagged events.

$\sigma_{\gamma^*\gamma^*}$: MC comparison

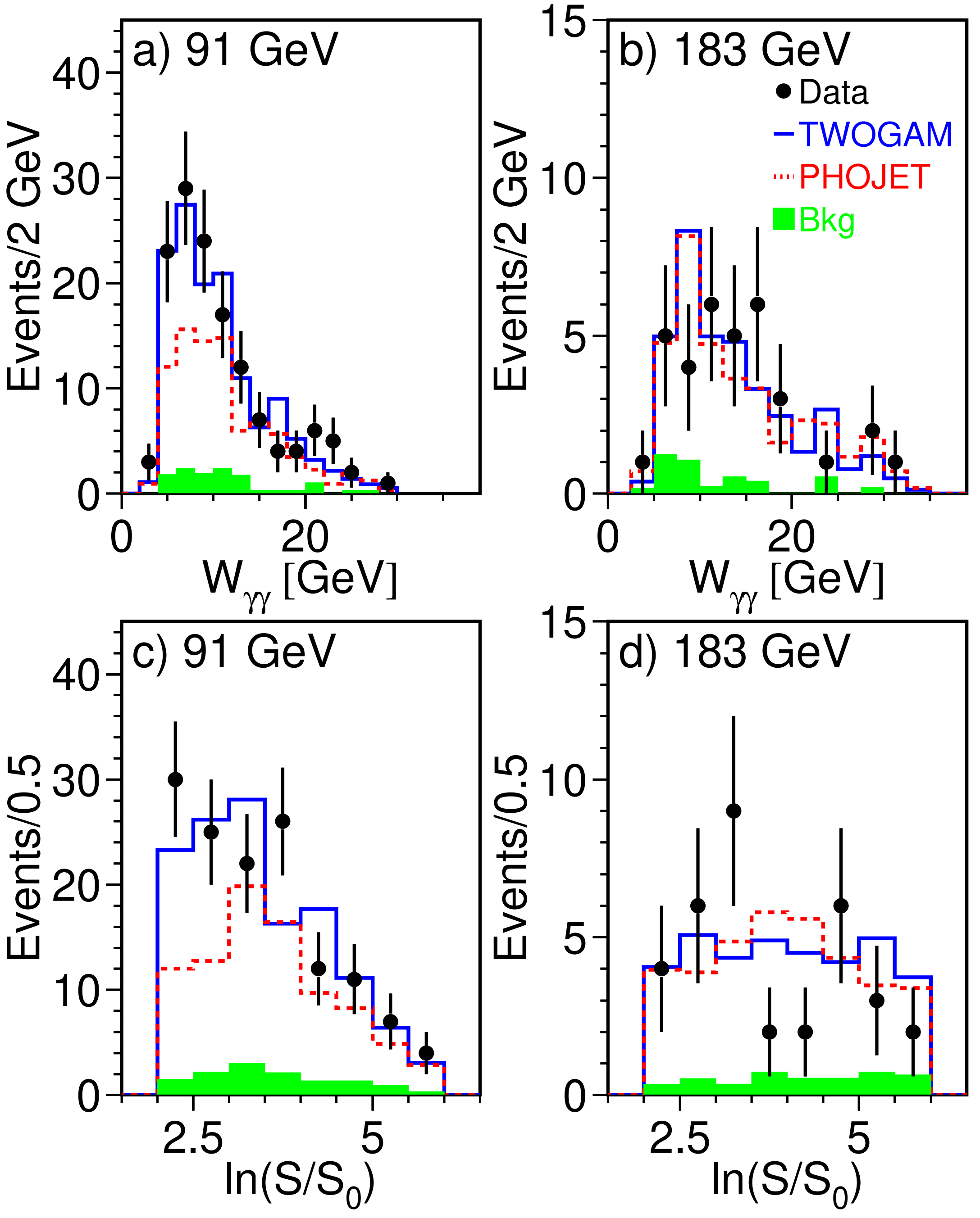

- **TWOGAM** **describes the data well at both energies.**
- **PHOJET is lower than the data in the low mass region at 91 GeV.**

$\sigma_{\gamma^*\gamma^*}$: Results

- **BFKL** calculation is more reliable at high Q^2 and high $W_{\gamma\gamma}$.
- the kinematic region is limited by :
  - ➪ $E_{tag} > 30$ GeV and 30 mrad $< \theta_{tag} <$ 66 mrad
  - ➪ $Q^2 > 2.5$ GeV^2 and $y \geq 0.1$
  - ➪ $2 < \ln(s/s_0) < 6$
- Number of events :

  91 GeV ➪ 12 events ($\varepsilon = 91\%$, $bkg = 5.9\%$)

  183 GeV ➪ 9 events ($\varepsilon = 86\%$, $bkg = 16\%$)
- $\sigma(\mathrm{e^+e^-} \to \mathrm{e^+e^-}\gamma^*\gamma^* \to \mathrm{e^+e^-} + hadrons)$:

	91 GeV	183 GeV
Data	$0.084 \pm 0.026 \pm 0.005$ pb	$0.17 \pm 0.07 \pm 0.01$ pb
BFKL	2.829 pb	2.135 pb
gluon	0.200 pb	0.135 pb
QPM	0.032 pb	0.018 pb
TWOGAM	0.089 pb	0.28 pb
PHOJET	0.066 pb	0.25 pb

*QPM is estimated by the program of Vermaseren with $m_u = m_d = m_s = 0.325$ GeV and $m_c = 1.6$ GeV.
*The prediction of BFKL Pomeron and gluon exchange is provided by Dr. A. De Roeck.

- PHOJET and TWOGAM agree with the data.
- The measured cross-section is much lower than the BFKL Pomeron prediction. ➜ the effect of NLO term ?!
- QPM is too low and the gluon exchange is compatible with the data at 183 GeV.

❑ Total cross-section of $\gamma\gamma$ collisions :

- ➪ The cross-section is measured for 5 GeV $\leq W_{\gamma\gamma} \leq$ 145 GeV.
- ➪ The cross-section increases at high energy ➜ independent of MC !
- ➪ The fitted value of ε, 0.16 ± 0.03, is larger than PDG value, 0.079.
  ➜ contribution from hard Pomeron !?
- ➪ The dominant uncertainty is the modelling dependence.
  ➜ L3 and OPAL are consistent if they use the same MC.
- ➪ The inclusive charged particle production of $\gamma\gamma$ collision is compatible with the NLO calculation and the p_T spectrum is much harder than in γp and (π, K)p interactions.

❑ Inclusive charm production :

- ➪ The measurement is done at 91 GeV $\leq \sqrt{s} \leq$ 183 GeV.
- ➪ The cross-section increases with increasing beam energy.
- ➪ The cross-section needs resolved processes (gluon content of photon) and larger than QPM model.

❑ Hadronic Photon Structure Function :

- The hadronic photon structure function, $F_{2,\mathrm{QCD}}^{\gamma}$, is measured for $1\ \mathrm{GeV}^2 < Q^2 < 2400\ \mathrm{GeV}^2$ and $0.002 < x < 1$.
- The dominant uncertainty is the modelling dependence.
  ➜ L3 and OPAL are consistent if using the same MC.
- At low x, the data lie between LAC1 and GRV-LO.
  ➜ Gluon density is overestimated in LAC1 and underestimated in GRV and SaS-1d.
- At high x, the agreement between the data and different models is good.
- The data is consistent with $\ln Q^2$ evolution.
- At high Q^2, the QPM model is insufficient at low x.
  ➜ need resolved processes.

❑ Leptonic Photon Structure Function :

- The measured values of $F_{2,\mathrm{QED}}^{\gamma}$ agree well with the QED calculation including non-zero photon virtuality and radiative corrections.
- The effect of longitudinal photons is small, but seen clearly in the azimuthal correlations

- **Cross-section of $\gamma^*\gamma^*$ collisions :**
  - **The cross-section is measured at $\sqrt{s} \simeq 91$ GeV and $\sqrt{s} \simeq 183$ GeV.**
  - **The data is much lower than the BFKL Pomeron prediction.**
  - **The QPM model is too small to describe the data.**

- **LEP will run until year 2000 ➜ the more data are coming !**

Even more precise results are foreseen !